Modeling the migration of fallout radionuclides to quantify the contemporary transfer of fine particles in Luvisol profiles under different land uses and farming practices

M. Jagercikova, O. Evrard, J. Balesdent, I. Lefevre, S. Cornu

Modeling the migration of fallout radionuclides to quantify the contemporary transfer of fine particles in Luvisol profiles under different land uses and farming practices

M. Jagercikova[a], O. Evrard[b], J. Balesdent[a], I. Lefèvre[b], S. Cornu[a]

a- INRA, UR1119 Géochimie des Sols et des Eaux, F-13100 Aix en Provence, France (Marianna.Jagercikova@aix.inra.fr; scornu@aix.inra.fr)

b- Laboratoire des Sciences du Climat et de l'Environnement (LSCE/IPSL), UMR8212 (CEA-CNRS-UVSQ), Domaine du CNRS, F-91198 Gif-sur-Yvette Cedex, France (olivier.evrard@lsce.ipsl.fr)

Corresponding author: M. Jagercikova, Marianna.Jagercikova@aix.inra.fr, +33 ø4 42 90 85 43

Abstract

Soil mixing and the downward movement of solid matter in soils are dynamic pedological processes that strongly affect the vertical distribution of all soil properties across the soil profile. These processes are affected by land use and the implementation of various farming practices, but their kinetics have rarely been quantified. Our objective was to investigate the vertical transfer of matter in Luvisols at long-term experimental sites under different land uses (cropland, grassland and forest) and different farming practices (conventional tillage, reduced tillage and no tillage). To investigate these processes, the vertical radionuclide distributions of ^{137}Cs and ^{210}Pb (xs) were analyzed in 9 soil profiles. The mass balance calculations showed that as much as 91 ± 9 % of the ^{137}Cs was linked to the fine particles (≤ 2 μm). To assess the kinetics of radionuclide redistribution in soil, we modeled their depth profiles using a convection-diffusion equation. The diffusion coefficient represented the rate of bioturbation, and the convection velocity provided a proxy for fine particle leaching. Both parameters were modeled as either constant or variable with depth. The tillage was simulated using an empirical formula that considered the tillage depth and a variable mixing ratio depending on the type of tillage used. A loss of isotopes due to

soil erosion was introduced into the model to account for the total radionuclide inventory. All of these parameters were optimized based on the ^{137}Cs data and were then subsequently applied to the ^{210}Pb (xs) data. Our results show that the ^{137}Cs isotopes migrate deeper under grasslands than under forests or croplands. Additionally, our results suggest that the diffusion coefficient decreased with depth and that it remained negligible below the tillage depth at the cropland sites, below 20 cm in the forest sites, and below 80 cm in the grassland sites.

Keywords: soil; lessivage; bioturbation; tillage practices; ^{137}Cs; ^{210}Pb (xs)

1. Introduction

Pedogenesis is a non-linear process in time and space (Montagne et al., 2013). Although the occurrence of major pedogenic processes can be easily identified in soil, their chronological succession and their rates are difficult to quantify due to the difficulty of finding relevant tracers to investigate the processes of interest in the appropriate temporal scale. Among these processes, lessivage, which is defined as the migration of fine particles ($\leq$ 2 µm or lutum fraction) from subsurface horizons (eluviation) and their accumulation in the B horizon (illuviation), has not been quantified, and its kinetics remain poorly understood (Quénard et al., 2011).

Lessivage was traditionally described as occurring at a timescale ranging from tens to thousands of years (Jamagne, 1973; Finke and Hutson, 2008). Although some authors considered that lessivage is an ancient pedogenic process that occurred exclusively under warm and humid climates (Jamagne, 1978; Jamagne et Pédro, 1981), Fedoroff (1997) showed that it is still currently active in regions with a Mediterranean climate. Therefore, we decided to study i) the

48 occurrence of current lessivage in a non-Mediterranean temperate climate and ii) the impact of
49 land use and agricultural practices on this lessivage.
50 Lessivage is considered to be the major pedogenic process occurring in several soil types
51 (Bockheim and Gennadiyev, 2000), mainly in European Luvisol and Albeluvisol soils. These
52 soil types are also particularly widespread in the USA and in China as they develop in all loess
53 deposits. In Europe, these soils cover 20 % of the surface (Jones et al., 2005). Several authors
54 hypothesized that agricultural activities could have a crucial impact on their evolution (Khan et
55 al., 2005; Kühn, 2003; Fedoroff, 1997). Therefore, they represent an ideal case study.
56 Lessivage is not the only pedogenic process that affects vertical solid matter transfers in soils.
57 Other processes that may act in synergy or in opposition to lessivage must be considered.
58 Pedoturbation processes, such as clay shrinking-swelling cycles, soil freezing and bioturbation,
59 tend to mix or, conversely, to segregate soil matter. Bioturbation is the movement of matter in
60 the soil due to the presence of living organisms (Gobat et al., 1998), soil fauna and/or root
61 systems, as well as tree falls (Wilkinson et al., 2010). This has several important consequences
62 on soil structure, such as the mechanical loosening of the soil, the oxygenation of the deepest
63 layers, the redistribution of organic matter, the transport of buried elements to the surface and the
64 neutralization of the pH. In all, it is clear that bioturbation plays an essential role in clay
65 distribution in soils. Although there are many agents that act in bioturbation, in a temperate
66 climate, earthworms are considered to be the main actor (Müller-Lemans and van Dorp, 1996;
67 Gobat et al., 2004; Persson et al., 2007), particularly anecic worms when vertical movement is
68 considered (Persson et al., 2007).
69

70 The fallout radionuclides ^{137}Cs and ^{210}Pb (xs) have different sources in the environment. ^{137}Cs
71 was released and dispersed during the nuclear weapon tests that occurred between 1953 and the
72 1970s, as well as by nuclear power plant accidents (Chernobyl in 1986 and Fukushima Dai-ichi
73 in 2011). In contrast, ^{210}Pb is naturally present because it is a product of ^{238}U decay and is a
74 daughter product of gaseous ^{222}Rn. Some ^{222}Rn may escape from the soil and lithosphere and
75 continue to decay in the atmosphere, resulting in ^{210}Pb, which then returns to the Earth's surface
76 through wet fallout. Therefore, this is referred to as unsupported or excess (xs) ^{210}Pb, in contrast
77 to supported ^{210}Pb that is naturally present in the soil. The fallout radionuclides ^{137}Cs and
78 ^{210}Pb (xs) have been used as tracers in soil studies because they are exclusively of atmospheric
79 origin. Furthermore, they are strongly sorbed to the soil solid phases: ^{137}Cs to clay particles
80 (Tamura and Jacobs, 1960; Sawhney, 1972; Cremers et al., 1988) and ^{210}Pb to clay particles and
81 organic matter (Dörr and Münnich, 1989). Thus, their transfer occurs only in association with the
82 solid matter in the soils that are not dominated by soluble organic matter transfers (Jarvis et al.,
83 2010; Matisoff et al., 2011). Finally, the choice of these radionuclides was also motivated
84 because their half-lives (30.2 years for ^{137}Cs and 22.3 years for ^{210}Pb) are favorable for
85 investigating the impact on the transfer processes due to modification in agricultural practices,
86 occurring at a decadal timescale.
87
88 These reasons justify the use of ^{137}Cs and ^{210}Pb (xs) as suitable tracers for estimating the kinetics
89 of solid matter transfer in soils, including lessivage and bioturbation. Diffusion-convection
90 modeling of the vertical distributions of these radionuclides (e.g., He and Walling, 1997;
91 Schuller et al., 1997) could provide a way to differentiate between these two processes because
92 the diffusion equation, which corresponds to the random mixing (or movement) of matter

upwards and downwards across short distances, is classically associated with bioturbation (Boudreau, 1986; Elzein and Balesdent, 1995; Schiffers et al., 2011), whereas convection as a long distance transport may be associated with lessivage. However, part of the long distance transport may also be associated with bioturbation, such as that resulting from the activity of anecic or epianecic earthworms. This bioturbation may result in more complex processes, such as litter incorporation into deeper layers or, reciprocally, deposits of deep horizon matter at the surface in the form of casts. In the diffusion-convection modeling, long-distance transport by bioturbation was assessed using a supplementary term (Jarvis et al., 2010). Other modeling approaches of worm mixing have been developed based on worm mixing experiments (Barnett et al., 2009; Schiffers et al., 2011). However, the experimental data provided by these studies show that they may be reasonably represented by a diffusion equation.

The aims of this study are (1) to quantify the current particle transfer by ^{137}Cs and ^{210}Pb (xs) in a soil sequence, as defined by Jenny (1941), considering human activity as a pedogenic factor (anthroposequences); (2) to determine the kinetics of these transfers by modeling the vertical distributions of ^{137}Cs and ^{210}Pb (xs) with a diffusion-convection equation using both constant and depth-dependent coefficients; and (3) to identify the impact of both land use and agricultural practices on the intensity and kinetics of particle transfer in soils.

2. Materials and Methods

2.1. Choice and description of the sampled sites

We selected three Luvisol sequences from Northern France that experienced different land uses (cultivation, grassland and forest), as land use impacts both the soil pH and the soil organic matter content, which are known to influence soil particle stability and dispersion (Le Bissonnais and Arrouays, 1997; Chenu et al., 2000). Additionally, two agricultural practices, manure input and tillage reduction were investigated because tillage reduction modifies the preferential flow paths in soils (Dexter, 1993), and this process was shown to be responsible for particle detachment (Majdalani et al., 2007).

These sequences were part of long-term experiments conducted to evaluate the impact of different farming practices on soil characteristics (Table 1). They also cover a gradient in pH (from 7 to 6) and in duration (from 40 to 11 years). The Luvisols developed on Weichselian loess deposits and have an age of 15-16 ka (Antoine et al., 2003); currently, these soils experience a temperate climate (Table 1). The three soils, described in Table 2, differ in depth. Mons's Luvisols were developed on several meters of loess and were, therefore, well drained, whereas clay and gritstone deposits were reached at approximately 1.5 m depth in the Feucherolles samples, and chalk was reached at approximately 80 cm depth in the Boigneville samples. The Luvisols in Feucherolles exhibit redoxic features due to a change in parent material at this depth. All sites were sampled in flat conditions (< 1 % slope). To be comparable within a given site, the three plots were closely situated and in equivalent topographic situations.

2.2. Soil sampling

Sampling was conducted in soil pits by continuous scraping of the soil with clean stainless steel tools. To avoid cross-contamination, the tools were cleaned and dried between each sampling level. Any soil that fell from the higher levels onto the sampling surface was carefully removed.

Each sample consisted of approximately 3 to 4 kg of bulk soil. The sampling was continuous, with varying sampling increments of 2 cm to 10 cm depth. The samples were then oven-dried at 40°C and sieved to 2 mm. The soil bulk densities were determined using the cylinder method for each horizon and using gamma-ray attenuation for surface horizons. The results of the pedologic analysis (the particle-size fractions, organic carbon, pH, exchangeable cations and bulk density) are summarized in Table 3.

2.2.3. Particle-size fractionation

Particles with diameters ≤ 2 μm were extracted from certain samples (at least one sample per horizon). These soil subsamples, weighing 150 g, were dispersed in 540 ml of de-ionized water with 20 agate beads (5 mm in diameter) via shaking for 22 h in an overhead shaker at a speed of 37 rpm. The organic-rich samples subsequently underwent ultrasonic dispersion. The ultrasonic dispersion was applied to 300 ml of suspension for 14 min, with 5 sec pulses every 9.9 sec. The samples remained continuously at cool temperatures to avoid damaging the clay particles with the released heat (Schmidt et al., 1999). The total energy dissipated into the suspension was *ca*. 200 J ml^{-1}.

The suspensions were allowed to settle according to Stokes' law. After sedimentation, the ≤ 2 μm fraction was sampled and centrifuged for 20 minutes at 10,000 rpm. The collected ≤ 2 μm fraction was then freeze-dried.

2.3. ^{137}Cs and ^{210}Pb analysis

The soil was packed into 60-ml pre-tared polyethylene specimen cups and sealed airtight to trap the ^{222}Rn and allow ingrowth of its decay products. The activities of ^{137}Cs (661.6 keV) and ^{210}Pb

(46.5 keV) were determined by gamma spectrometry using the very low-background HPGe detectors available at the *Laboratoire des Sciences du Climat et de l'Environnement* (LSCE, Gif sur Yvette, France). The ^{210}Pb (xs) activity was calculated by subtracting the supported activity from the total ^{210}Pb activity (Evrard et al., 2010).

The counting times of the soil samples varied between 8×10^4 and 3×10^5 s. All measured counts were corrected for background levels, which were measured at least every 2 months, as well as for the detector and geometry efficiencies. The results were systematically expressed in Bq kg^{-1}. The radionuclide activities were systematically decay-corrected according to the sampling date. The counting efficiencies and quality assurances were conducted using internal and certified IAEA standards that were prepared in the same specimen cups as the samples.

2.4. Numerical modeling

2.4.1. Convection-diffusion equation

The migration of fallout radionuclides in soil is classically described using a diffusion-convection equation (e.g., He and Walling, 1997; Schuller et al., 1997):

$$\frac{\partial A}{\partial t} = \frac{\partial}{\partial z}\left(D_s \frac{\partial A}{\partial z} - v_s A\right) - \lambda A \qquad (1)$$

where A is the total radionuclide activity per volume of soil (Bq m^{-3}; obtained by multiplying the measured activity in Bq kg^{-1} by the bulk density of the sample), z is the soil depth (m), t is the time (s), D_s is the diffusion coefficient of the solid phase (m^2 s^{-1}), v_s is the convection velocity (m s^{-1}), and λ is the radioactive decay constant (s^{-1}).

The diffusion coefficient D_s and the convection velocity v_s were assumed as constants with time in this study. Because true velocity coefficients are expected to vary slightly with time (Rosén et

al., 1999), our estimates of v_s (and possibly D_s) represent the weighted average coefficients over the 20 to 50 year period recorded by the two radionuclides. Although these coefficients are generally considered to be constant with depth in the literature (e.g., Smith and Elder, 1999; Bossew and Kirchner, 2004; Schimmack and Feria Márquez, 2006; among others), several authors have proposed that they are depth-dependent; therefore, we tested the use of variable coefficients in a second step (Elzein and Balesdent, 1995; Schuller et al., 2004).

2.4.2. Boundary conditions

A boundary condition of the injection of the radionuclides was applied at the soil surface. The injection of the radionuclides was obtained by multiplying the annual fallout deposition $a_0(t')$ in Bq m^{-2} during the considered year t' by Dirac delta function $a(0, t') = a_0(t')\delta(t-t')$:

$$D_s \frac{\partial A(0,t')}{\partial z} = a_0(t')\delta(t-t') \quad (2)$$

The isotopes were delivered to the surface either annually (^{137}Cs) or proportionally at every time-step (^{210}Pb (xs)). The input time-series were, therefore, treated as a time-dependent boundary condition: $A(0, t') = A(0, t'-1)+a_0(t')\delta(t-t')$.

For ^{137}Cs, all simulations began in 1954 and finished in the sampling year. The annual global fallout input $a_{GF}(t')$ followed the distribution calculated by Cambray et al. (1989), with a total fallout accumulation of 3018 Bq m^{-2} by 1986, prior to the Chernobyl accident. The ^{137}Cs input (a_{Ch}) due to the Chernobyl accident was determined using the empirical equation developed for France (Roussel-Debel et al., 2007). This equation takes into consideration the longitude of the sampling site and the mean cumulative rainfall recorded between the 1st and the 5th of May 1986. The obtained values for the Chernobyl fallout amounted to 661 Bq m^{-2} for Mons, 413 Bq m^{-2} for

206 Feucherolles and 499 Bq m^{-2} for Boigneville. The Fukushima Dai-ichi accident in 2011 led to
207 negligible ^{137}Cs fallout in France (*i.e.,* < 2 Bq m^{-2}; Evrard et al., 2012).
208 For ^{210}Pb (xs), the annual fallout (a_{Pb}) was considered constant over the last three centuries and
209 was determined using the optimization procedure. In the case of the forest, the simulations were
210 long enough to allow the ^{210}Pb (xs) to reach dynamic equilibrium between its input and
211 radioactive decay. In the case of the grassland, the simulation began in 1939, with an initial ^{210}Pb
212 (xs) vertical distribution identical to that recorded in the conventionally tilled plots.
213
214 The bottom boundary was set deep enough (at 200 cm) to avoid influencing the numerical
215 solution within the first 100 cm. We used an advective transport free of diffusion as a boundary
216 condition to avoid spurious accumulations of radionuclides.
217
218 **2.4.3. Modeling of mixing by tillage and erosion**
219 Tillage homogenizes the radionuclide concentrations within the tilled horizon. To separate the
220 bioturbation effect from the tillage effect, we modeled tillage at time $t + \Delta t$, where t stands for
221 the time just before the tillage and Δt for the time-step, using the following equation:

222 $$A(z,t+\Delta t) = (1-M_R)A(z,t) + \frac{M_R}{T_D}\int_0^{T_D} A(z,t)dz \qquad \forall\, z \in [0;T_D] \qquad (3)$$

223 where M_R is the mixing ratio and T_D is the tillage depth (m). M_R was set (depending on the tillage
224 practices) to 0.85 for conventional tillage and 0.30 for reduced tillage (according to Ullrich and
225 Volk, 2009); T_D ranged between 23 and 28 cm for conventional tillage and between 5 and 10 cm
226 for reduced tillage, depending on the history of the tillage practices for a given plot (Table 4). A
227 total erosion term, including water erosion induced by surface runoff and tillage, was included in
228 the modeling for the cropland plots. The erosion and the associated loss of radionuclides was

allowed to occur only in the upper cell of the modeled soil domain, representing the first 0.1 cm of soil, during the period without vegetal cover (October-February), using the following equation:

$$A(z,t+\Delta t) = (1-E)A(z,t) \qquad \forall z \in [0;0.1] \tag{4}$$

where E is the erosion parameter (in 10^{-3} cm). This parameter was adjusted using the fitting procedure and was subsequently expressed in terms of annual soil erosion both in mm yr^{-1} and t ha^{-1} yr^{-1} by multiplying the erosion parameter by the number of months with the erosion (five months) and by the surface soil bulk density. Consequently, erosion was determined by both the total inventory and the isotopic concentration at the surface, as well as its evolution with time. Therefore, with low radionuclide concentrations at the surface, substantial erosion would be estimated by the model. The modeling setups and initial parameters for each site are summarized in Table 4.

2.4.4. Discretization and resolution of the equation

We solved differential equation (1) using upstream finite difference approximations for the spatial derivatives and the semi-implicit Crank-Nicholson scheme as a time-solver. The obtained algebraic system of equations was solved by Gaussian elimination. The time-step was equal to 0.01 year. The accuracy of the numerical solution was verified by comparing it to the analytical solution with a single pulse-input a_0 in Bq m^{-2} at t=0 (5) (e.g., Schuller et al., 1997). The numerical scheme was conservative for the simulations without tillage. The inclusion of annual tillage generated a difference of 0.3 % in the total inventory at the end of the simulation.

$$A(z,t) = a_0 \left\{ \frac{1}{\sqrt{\pi D_s t}} \exp\left(-\frac{(z-v_s t)^2}{4 D_s t} \right) - \frac{v_s}{2D_s} \exp\left(\frac{v_s z}{D_s} \right) \operatorname{erfc}\left(\frac{v_s}{2}\sqrt{\frac{t}{D_s}} + \frac{z}{2\sqrt{D_s t}} \right) \right\} \exp^{-\lambda t} \tag{5}$$

2.4.5. Non-linear least squares minimization procedure

The unknown parameters ($D_s(z)$, $v_s(z)$, and E) and their standard deviations were determined using a non-linear least squares minimization procedure based on the Levenberg-Marquardt algorithm included in the Python *lmfit* package. The minimized value for each measurement A_m was calculated in integral form to account for the different sampling intervals (Bossew and Kirchner, 2004):

$$\text{argmin} = \left(A_m(z_2 - z_1) - \int_{z_1}^{z_2} A(z,t)dz\right)^2 \quad (6)$$

To estimate the performance of the fitting procedure, we calculated the residual sum of squares (*RSS*) for *N* sampled layers and the modeling efficiency (*EF*), with $\overline{A}_m$ being the mean A_m value:

$$RSS = \sum_{i=0}^{N} \left(A_m(i)(z_{i2} - z_{i1}) - \int_{z_{i1}}^{z_{i2}} A(z,t)dz\right)^2 \quad (7)$$

$$EF = 1 - \frac{\sum_{i=0}^{N} \left(A(z,t) - A_m(i)\right)^2}{\sum_{i=0}^{N} \left(A_m(i) - \overline{A}_m\right)^2} \quad (8)$$

EF can vary between -∞ and 1. An *EF* of 1 is a perfect match between the model and the measurements, whereas a negative *EF* value means that using the average value of the isotopic concentrations would produce a better representation of the isotopic concentrations than the optimized simulation.

3. Results and discussion

3.1. Estimation of erosion, lessivage and bioturbation rates based on the ^{137}Cs data

3.1.1. Inventories and ^{137}Cs depth distributions in bulk soil samples and the ≤ 2 µm size fraction

The maximum ^{137}Cs inventories were found under the grassland in Mons, the forest in Feucherolles and the conventional tillage in Boigneville (Table 5). Following the estimates of the Chernobyl fallout determined by Roussel-Debel et al. (2007) and the global fallout reported by Cambray et al. (1989), we observed an excellent match between the predictions of the ^{137}Cs deposition for the Mons and Feucherolles sites recalculated for the sampling year (2072 and 1932 Bq m^{-2}, respectively) and for the ^{137}Cs inventories measured in the Mons's grassland and Feucherolles's forest (Table 5). On average, 17 % of the present day ^{137}Cs contamination in the studied sites was supplied by the Chernobyl accident, and the rest was due to the nuclear weapon tests.

The inventories for the cultivated sites were lower than their natural equivalents (Table 5). Therefore, the cultivated sites were likely affected by soil erosion, which was reflected as a loss of ^{137}Cs compared to the theoretical inventory calculated from the reference sites.

In the cases of the grassland and forest, we observed peak-shaped ^{137}Cs vertical distributions with maximum isotopic concentrations in the A horizon (Fig. 1). The depths of maximum isotopic concentrations were 11 cm in the grassland and 13 cm in the forest. The vertical distributions in the cropland remained roughly homogeneous in the tillage horizon. In the cases of manure input and both reduced tillage plots, we observed the maximum below the tillage depth. The no tillage experiment showed two barely distinguishable maxima at 5 cm and 13 cm.

The deepest ^{137}Cs penetration could be differentiated between the undisturbed and cultivated sites. Under permanent vegetation, ^{137}Cs penetration was due to pedological processes. The penetration reached 50 cm depth in the grassland and 40 cm depth in the forest. In the agricultural sites, this penetration was controlled by the tillage depth after the main ^{137}Cs input, as displayed by the sharp gradient in concentration at the lower limit of the tillage layer. In Feucherolles, this depth corresponded to 40 cm, whereas it reached 37 cm in Mons, independent of the different treatments. Additionally, in Boigneville, the depth of ^{137}Cs penetration varied slightly depending on the tillage practice, as described in the following sequence: conventional tillage (35 cm) > reduced tillage (31 cm) > no tillage (30 cm). The mass balance calculation showed that there was a similar amount of soil within the upper 35 cm under the conventional tillage sites, within the upper 31 cm under the reduced tillage sites and the upper 30 cm under the no tillage sites. This may be interpreted as a result of soil compaction due to tillage reduction, and this phenomenon has already been described by Dimassi et al. (2013). Therefore, the maximum penetration depth under agricultural sites was related to the maximum tillage depth before the start of the long-term experiment but after the majority of the ^{137}Cs was supplied by global fallout.

We measured the ^{137}Cs activities in the ≤ 2 µm size fractions for a selection of 25 samples. Using the data for particle-size distributions, we calculated the contribution of the ^{137}Cs activity borne by the ≤ 2 µm fraction to the bulk sample activity (Table 6). This contribution was, on average, 87 ± 10 % in Mons, 94 ± 6 % in Feucherolles and 95 ± 10 % in Boigneville. Therefore, we conclude that ^{137}Cs is predominantly associated with the ≤ 2 µm size fraction in the soils of the

317 studied sites and confirm that ^{137}Cs effectively tracks the transfers of this particle size fraction
318 within the soil profile.
319
320 **3.1.2 Modeling of ^{137}Cs vertical distributions with constant coefficients**
321 In the grassland, forest and no tillage experiments, the diffusion coefficients were relatively high
322 (Table 7), and diffusion was the main mixing process. For the cultivated plots (with the
323 exception of the no till experiment), however, we obtained diffusion coefficients lower than 0.01
324 $cm^2\ yr^{-1}$. We conclude that both conventional and reduced tillage induced such a large degree of
325 mixing that diffusion was masked in the isotopic distribution profiles and that the model was
326 thus unable to determine the respective contributions of the two processes. Therefore, the
327 cultivated plots were modeled without diffusion. These simulations performed well (Table 7),
328 yielding *EF*s ranging between 0.97 and 0.99 and a good fit to the data below the tillage depths.
329 The convection rates in all plots ranged from 0.08 to 0.29 cm yr^{-1}, with a mean value of 0.16
330 cm yr^{-1} (Table 7). The highest v_s coefficient was observed under the grassland sample (0.29 ±
331 0.02 cm yr^{-1}). Similar convection velocities, varying between 0.15 and 0.28 cm yr^{-1} (a mean of
332 0.21 ± 0.05 cm yr^{-1}), were obtained for grassland Luvisols in Bavaria (Schimmack and Feria
333 Márquez, 2006). For the sites under cultivation, the v_s coefficients were higher in Boigneville
334 than in the two other sites; the v_s decreased with tillage in Boigneville but not in Mons, which
335 experienced a shorter duration of tillage reduction. Additionally, the v_s increased with manure
336 input. The v_s coefficients were similar between the forest and conventional tillage plots. For the
337 forest site, the obtained *EF* was rather poor (*EF*=0.78), and the model clearly underestimated the
338 ^{137}Cs concentrations below 25 cm (Fig. 2). The forest site was, therefore, a good candidate to test
339 the impact of variable coefficients with depth.

340

341 **3.1.3 Modeling of ^{137}Cs vertical distributions with variable coefficients**

342 We successively tested the following scenarios: i) exponentially decreasing the diffusion
343 coefficient and ii) changing the convection velocity based on segments lines with endpoints at
344 characteristic depths.

345

346 *Exponential decrease in the diffusion and constant velocity for the grassland, forest and the no*
347 *till experiments*

348 The mixing in soils described by the diffusion equation is classically interpreted as
349 corresponding to the bioturbation activity (e.g., Elzein and Balesdent, 1995; Schiffers et al.,
350 2011). Bioturbation depends on organic matter distribution, which is consumed by bioturbating
351 organisms. Therefore, we decided to model the evolution of the diffusion coefficient with depth
352 as the evolution of organic matter, which decreases exponentially with depth. We considered an
353 exponential evolution for $D_s(z)=D_0\exp(-bz)$, with the parameters D_0 and b to be optimized during
354 the fitting procedure.

355 The modeling efficiency *EF* for the models with exponentially decreasing diffusion improved
356 from 0.96 to 0.97 for grassland, from 0.78 to 0.87 for forest and from 0.80 to 0.95 for the no till
357 samples compared to the models with a single value for diffusion (Table 7). For the forest site,
358 the diffusion coefficient was high at the surface and rapidly decreased with depth, becoming
359 insignificant below 20 cm (Table 7). For the grassland, the diffusion was lower than that of the
360 forest at the surface, but it slowly decreased with depth, approaching zero only below 80 cm.

361 We calculated the mean diffusion in the first 30 cm, and the results were as follows: 4.78 ± 12.39
362 $cm^2\ yr^{-1}$ under forest; 3.16 ± 1.92 $cm^2\ yr^{-1}$ under grassland and 3.33 ± 7.73 x 10^{-5} $cm^2\ yr^{-1}$ under

363 the no till plot. These values and the associated uncertainties remained similar to the values
364 found when using the constant diffusion model (Fig. 3). For the no till experiment, the mean
365 diffusion remained unreasonably low, inducing a very narrow peak at 3 cm depth in the ^{137}Cs
366 depth distribution (Fig. 1). A potential explanation for the difficulty in quantifying the diffusion
367 in this plot might be that some ^{137}Cs had already been substantially redistributed by tillage before
368 1970. However, the low diffusion in the no till treatment is in accordance with the very sharp
369 carbon gradient that was developed and maintained in the upper 10 cm throughout the 41 years
370 of treatment at Boigneville (Fig. 2).
371
372 *Variable diffusion and variable convection velocity*
373 Because organic matter stabilizes clay particles (Chenu et al., 2000), we considered that it most
374 likely decreases the convection velocity. Similarly, we assumed that pH influenced this velocity
375 and, therefore, that the convection velocity varied with depth as a function of these two
376 pedologic characteristics of the soil (Fig. 2). The effects of pH variations on the convection
377 velocity were considered using the IMC_{pH} indicator defined by Van Breemen and Buurman
378 (2002), which varies between 0 and 1, where 1 indicates likely clay migration, and 0 indicates
379 low probability of migration. We estimated that the organic matter content controlled convection
380 velocity between 0 and 20 cm, within the depth range where the IMC_{pH} generally had a value of
381 1 (Fig. 2). In the case of conventional tillage, where the organic matter content was low, we
382 hypothesized that the IMC_{pH} would more likely impact the evolution of convection velocity, with
383 changes occurring below 40 cm depth in Mons and Feucherolles and below 20 cm in
384 Boigneville. The transition zones of these parameters were chosen as the endpoints of the
385 segment lines for modeling simplicity (Table 4).

386 Compared to the model with constant convection velocity, the modeling efficiency *EF* improved
387 at most sites, although three sites already had an *EF* value of 0.99 (Table 8).
388 The calculated averages of variable diffusion parameters were not significantly different from the
389 ones found for the constant convection velocity models (Fig. 3). In the no till experiment,
390 diffusion was still very low.
391 The obtained convection velocities increased under conventional tillage (manure input included)
392 and in the grassland for the 0-20 cm and 0-40 cm zones, respectively. At 40 cm depth, the
393 convection velocity ranged between 0.16 and 0.29 cm yr^{-1} for conventional tillage, while it
394 decreased for the grassland.
395 For the reduced tillage in Mons and the Feucherolles forest, the convection velocity decreased in
396 the 0-20 cm range, followed by a slight increase in the 20-40 cm range in Mons under reduced
397 tillage; however, there was a sharp increase in the 20-40 cm range in the forest of Feucherolles.
398 The convection velocity at the surface under reduced tillage was significantly higher (v_s=0.23 ±
399 0.05 cm yr^{-1}) than that under conventional tillage in Mons. In contrast, in the reduced tillage
400 experiments (including no tillage) in Boigneville, the convection velocity did not change with
401 depth.
402 Finally, despite the important uncertainties, the simulation of the concentrations below 25 cm
403 depth improved with the variable velocity parameters, justifying the use of such parameters.
404 The mean velocity in the first 40 cm had much higher uncertainties with the variable velocities
405 (276 % on average) than with the constant velocities (8% in average) (Fig. 3), principally due to
406 error propagation. In the cultivated areas, the mean convection velocity of depths greater than 40
407 cm was not significantly different between the constant and variable parameters. In the grassland
408 and forest, however, the mean variable convection velocities in the first 40 cm were larger with

409 the convection velocities that varied by depth than with the constant convection velocities
410 (Tables 7 and 8). The uncertainties associated with the variable convection model for these sites
411 were among the most important.
412
413 **3.1.4. Erosion rates**
414 Simulated and calculated erosion did not significantly change between the constant and variable
415 convection velocities and ranged between 1.81 to 9.80 t ha^{-1} yr^{-1} (Fig. 3).
416 The erosion rates decreased from Mons to Feucherolles to Boigneville. The tillage reduction, as
417 well as manure input, lowered the erosion rate, notably in Mons. These trends are in agreement
418 with the literature, and the global erosion rates were consistent with ones reported for Western
419 Europe, such as *ca.* 1-5 t ha^{-1} yr^{-1} for erosion due to runoff (Cerdan et al., 2010) and 3.3 t ha^{-1} yr^{-1}
420 due to tillage erosion (Van Oost et al., 2009). The highest erosion rates, which were obtained in
421 Mons, might be related to the inclusion of sugar beet cultivation in the crop rotation, which
422 enhances runoff and erosion (Evrard et al., 2008). Furthermore, sugar beet harvest is known to
423 export significant quantities of soil (Poesen et al., 2001).
424
425 **3.2. Validation of the diffusion and convection velocity coefficients with the ^{210}Pb (xs) data**
426
427 **3.2.1. Inventories and ^{210}Pb (xs) vertical distributions in the bulk soil samples and the ≤ 2**
428 **µm size fraction**
429 The ^{210}Pb (xs) activities were larger than the limit of quantification only in 29 of the 113 samples
430 (Supplementary data file). In all other samples (84 of the 113), we could not discern any
431 significant activity of ^{210}Pb (xs) due to very small differences between the total and supported

^{210}Pb (xs) (~3 Bq kg^{1}). Despite these high uncertainties, we observed some general trends in the vertical ^{210}Pb (xs) distributions. The ^{210}Pb (xs) concentrations were detected down to 20 cm in the grassland, with a total inventory of 1548 ± 1377 Bq m^{-2}. Higher concentrations were measured in the forest, and the radionuclide was detected down to a depth of 14 cm, with a total inventory of 1921 ± 1959 Bq m^{-2}. The maximum isotopic concentrations of ^{210}Pb (xs) were found at the soil surface, with the exception of the manure plot, where the maximum concentrations were measured at 20 cm. The three plots under conventional tillage displayed ^{210}Pb (xs) concentrations below the detection limit at all depths due to dilution generated by the tillage. Under reduced tillage, the ^{210}Pb (xs) concentrations were detected only in the upper 10 cm and only in the upper 4 cm in the no till experiment. Because of the larger uncertainties associated with the ^{210}Pb (xs) data, we decided to test whether the D_s and v_s values determined by the ^{137}Cs vertical distributions would fit the ^{210}Pb (xs) data only for the grassland and the forest.

Isotopic concentrations of ^{210}Pb (xs) in the ≤ 2 μm size fraction were detected in 19 of the 25 samples (Table 6). For 8 samples collected below 4 cm depth, ^{210}Pb (xs) was detected in the ≤ 2 μm size fractions, even though concentrations remained below the detection limits in the bulk soil samples. The ^{210}Pb (xs) concentrations in the ≤ 2 μm size fraction, relative to the bulk samples, were 65 ± 14 % on average for the surface samples (range from 0 to 4 cm n=7) and 129 ± 16 % on average for the deeper samples (n=4). Therefore, we conclude that, in the surface samples (0-4 cm), a portion of the ^{210}Pb (xs) was sorbed by particles coarser than 2 μm, but at deeper levels, the ^{210}Pb (xs) was predominantly associated with the ≤ 2 μm size fraction. The ^{210}Pb (xs) content of the size fraction coarser than 2 μm linearly increased with increases in the organic carbon content of this fraction (Fig. 4). This observation suggests that the ^{210}Pb (xs) that

455 was not contained in the ≤ 2 µm fraction may be linked to coarse organic matter particles. This
456 corroborates the conclusions of Dörr and Münnich (1989), suggesting that organic matter
457 controls the migration of ^{210}Pb (xs) in the soil.
458
459 **3.2.2. Modeling of ^{210}Pb (xs) vertical distributions and its signification**
460 The fitting of the ^{210}Pb (xs) depth distribution estimated a flux of ^{210}Pb (xs) of 93 ± 8 Bq m^{-2} yr^{-1}
461 for the grassland and 83 ±18 Bq m^{-2} yr^{-1} for the forest site, which is similar to the estimation of
462 the mean ^{210}Pb flux of 117 Bq m^{-2} yr^{-1} over continents in the 30°-60° N latitudinal band (Preiss et
463 al., 1996). However, the simulations fit the data poorly, as shown by the low modeling
464 efficiencies (*EF*) (lower than 0.5 for all land uses considered). The variable velocity model failed
465 to reproduce the surface peak of the forest plot, though the simulation with constant velocity
466 performed better (Fig. 5). As discussed above, a portion of the ^{210}Pb (xs) in this layer is bound to
467 organic matter particles larger than 2 µm that were most likely not transferred by lessivage. We
468 therefore conclude that ^{210}Pb (xs) in the bulk soil might not be a suitable tracer for lessivage. We
469 modeled the ^{210}Pb (xs) activities measured in the ≤ 2 µm size fractions for the forest. In that case,
470 the simulation with variable convection velocity was more satisfactory, with an *EF* improving
471 from -0.02 to 0.67. Due to the low number of samples and the poor modeling efficiency, we
472 conclude that the depth distribution of ^{210}Pb does not invalidate the parameters of solid matter
473 transfer that were calculated from the ^{137}Cs profiles.
474
475 **3.3. Estimation of bioturbation and modern lessivage rates with radionuclides:**
476 **contribution and limitations**
477

3.3.1. Comparison of movement parameters and bioturbation between permanent vegetation and cultivated sites

Bioturbation is generally addressed as the amount of matter ingested by macrofauna (mainly the earthworm in temperate climates) per year in the uppermost 30 cm of the soil (Gobat et al., 2004). To express the diffusion in terms of bioturbation, we followed the approach described by Jarvis et al. (2010), who described the relationship between diffusion and the ingestion rate, taking into account the soil bulk density and the body length of earthworms. In our case, we estimated the earthworm ingestion rates over the first 30 cm of the soil from the mean diffusion over the same depth (calculated with depth dependent variable diffusion) and the body length of earthworms (8 to 10 cm for sites with permanent vegetation and 5 cm length for no till experiment plot). Because of important uncertainties associated to the surface diffusion term for the forest, the bioturbation was not evaluated for this plot. For the no till experiment plot, we used the value found with constant diffusion (0.13 $cm^2\ yr^{-1}$) because the value obtained with the variable coefficient was considered too low. For body lengths of 10 cm and 8 cm, we obtained ingestion rates of 147 and 229 $kg\ m^{-3}\ yr^{-1}$ and soil turnover rates of 0.11 and 0.17 yr^{-1}, respectively, for the grassland. For the no till experiment, the ingestion rate was 59 $kg\ m^{-3}\ yr^{-1}$, with a soil turnover rate of 0.04 yr^{-1}. By integrating the ingestion rates over the upper 30 cm, we calculated the associated mean bioturbation of this layer to be 441 and 687 $t\ ha^{-1}\ yr^{-1}$ for the grassland and 177 $t\ ha^{-1}\ yr^{-1}$ for the no till experiment. The latter result is remarkably consistent with the value of 126 $t\ ha^{-1}\ yr^{-1}$ estimated by the ecological studies of earthworm biomass at the studied site (Cluzeau, pers. communication). Unfortunately, we did not benefit from similar studies for our grassland and forest sites. Therefore, we summarized the estimates of bioturbation and surface cast rates for grasslands and deciduous forests in humid temperate climates from the

501 literature (Table 9). The range of bioturbation rates is extremely large, especially in grasslands.
502 Our results are the same order of magnitude as published results for grasslands. Obviously,
503 inferring solid matter transport rates from earthworm ingestion rates would be improved by
504 estimating the average distance of soil transport by the organisms, which depends on their
505 ecological categories (*i.e.,* anecic, epianecic or endogeic). Some bioturbation processes may also
506 lead to convection-like transport. Litter or A horizon incorporation into deep layers by anecic
507 earthworms or downward movement via vertical galleries or root holes may transport topsoil
508 downwards. Reciprocally, the deposition of deep horizon matter at the surface as casts, such as
509 that performed by anecic earthworms or termites, may help bury the A horizons, a process which
510 would contribute to a uniform downwards movement of the intermediate layers. Thus, the mean
511 velocity over the 0-40 cm layer in the forest and grassland soils (approximately 0.5 cm yr^{-1};
512 Table 8) may represent a quantitative estimate of such biological "burial" activity.
513 Finally, while tillage homogenizes the isotopic concentrations within the tilled horizon, it creates
514 an important concentration gradient at the lower boundary of this layer that allows the
515 investigation of the local transfer rates at this depth. Because the implementation of the diffusion
516 process was not necessary for modeling conventional and reduced tillage, we conclude that the
517 diffusion process is negligible below the depth of conventional tillage (25-28 cm) during the
518 investigated timescale. At this depth, the diffusion was of ~1.99 cm^2 yr^{-1} for the grassland, but
519 was negligible for the forest.
520
521 **3.3.2. Impacts of pedologic characteristics on modern lessivage**
522 Because ^{137}Cs and ^{210}Pb (xs) are mainly sorbed on the fraction ≤ 2 μm, their transfer in the soil
523 by convection may represent the lessivage of fine particles. These isotopes are mainly present in

524 the A horizons, and they effectively trace the particle transport from the A to the E horizons (*i.e.,*
525 eluviation). According to the simulations with the depth-dependent variable coefficient, lessivage
526 is more active in the grassland and the forest than in areas under cultivation (higher v_s, Fig. 3),
527 which is consistent with their high IMC_{pH} (equal to 1) over the upper 40 cm. For areas under
528 cultivation, this indicator is either lower than 1 or equal to 1 at a maximum depth of 20 cm.
529 Reducing tillage did not influence lessivage in Mons, but it did reduce lessivage in Boigneville.
530 Because Mons only experienced 11 years of tillage reduction while Boigneville experienced 42
531 years, the apparent difference in the action of tillage reduction on lessivage may be due to the
532 difference in duration. The slowing of lessivage when tillage is reduced is consistent with the
533 increase in structural stabilization observed when the tillage intensity decreases (Le Bissonnais
534 and Arrouays, 1997).
535 To compare these convection velocities to the concentrations of particles migrating through soils
536 measured in a column experiment in the literature (see synthesis by Quénard et al., 2011), we
537 calculated the annual flux of particles (f in g cm^{-2} yr^{-1}) over the upper 40 cm for the grassland,
538 and we divided it by the annual drainage (estimated as the difference between annual rainfall and
539 the potential evapotranspiration).
540 The annual flux of particles was estimated using the following equation:
541 $$f(z)=v_s(z)a_D(z) \qquad (9)$$
542 where v_s is the convection velocity estimated from the ^{137}Cs data (Table 8) and a_D is the quantity
543 of available ≤ 2 μm fraction (in g cm^{-3}) for particle transfer at a given depth, which is calculated
544 as follows:
545 $$a_D=\rho d C_{<2\mu m} \qquad (10)$$

546 where ρ is the bulk soil density (g cm^{-3} Table 3*), $C_{<2\mu m}$* is the ≤ 2 µm particle-size fraction (g g^{-1},
547 Table 3) and *d* is the fraction of the ≤ 2 µm size fraction surrounding the macropores (considered
548 available for particle transfer). Based on the hydraulic properties determined for this soil (data
549 not shown) and by defining macropores either as pores larger than 150 µm or as pores larger than
550 8 µm, we estimated that the macroporosity of this soil corresponds either to 1 % or 22 % of the
551 total porosity, depending on the assumed threshold. The relative abundance of the ≤ 2 µm
552 particles surrounding the macropores was considered to be proportional to the relative abundance
553 of the macropores, as proposed by Finke (2012). The obtained flux of particles ranged from
554 0.57×10^{-3} to 12.8×10^{-3} g cm^{-2} yr^{-1}. The average drainage calculated for this site for the last 30
555 years, based on data provided by Meteo France (Safran grid), was 103 mm yr^{-1}. Therefore, we
556 estimated that the obtained convection velocity corresponds to concentrations of the ≤ 2 µm
557 particles in the soil water ranging from 0.06 to 1.24 g L^{-1}. These concentrations are of the same
558 order of magnitude as the concentrations measured in the soil column experiments performed by
559 Jacobsen et al. (1997), Kjaergaard et al. (2004) and Cornu et al. (2014).
560
561 **5. Conclusions**
562
563 We investigated the vertical distribution of two fallout radionuclides (^{137}Cs and ^{210}Pb (xs)) in 9
564 Luvisol profiles from northern France to determine the impact of variable organic matter content,
565 pH and farming practices on the vertical transfer of solid matter in the soils, particularly by
566 bioturbation and lessivage. The ^{137}Cs mass balance calculations showed that as much as 91 ± 9
567 % of the ^{137}Cs was linked to the ≤ 2 µm size fraction, thus implying that ^{137}Cs is a valid tracer for
568 quantifying solid matter transfers in these soils. To model these processes, bioturbation was

569 estimated by calculating diffusion coefficients and lessivage was quantified by calculating
570 convection velocity coefficients. In the model, both coefficients were considered either as
571 constant or variable with depth. Tillage was represented by a mixing equation, and we added a
572 soil erosion term to fit with the measured inventories. The simulations greatly improved when
573 the variable coefficients were used, especially for the forest. Our modeling attempts showed that
574 diffusion could not be quantified when tillage was implemented, thereby demonstrating that the
575 large impact of tillage overshadows diffusion. We showed that the diffusion, and therefore
576 bioturbation, was negligible below the tillage depth in the cultivated sites, below 20 cm in the
577 forest and 80 cm in the grassland. The measured diffusion coefficients, when converted to
578 earthworm ingestion rates for the upper 30 cm, corresponded to 441 and 687 t ha^{-1} yr^{-1} for the
579 grassland. The mean convection velocities in the upper 40 cm ranged between 0.06 and 0.59
580 cm yr^{-1} and varied according to the following decreasing sequence: forest = grassland >
581 conventional tillage > reduced tillage = no tillage. However, it is important to note that we traced
582 the release of particles from the surface (eluviation) rather than their accumulation (illuviation).
583 The transfer coefficients obtained using the ^{137}Cs data were applied to the ^{210}Pb (xs) distributions
584 in the second step. The simulations performed only moderately well, and the surface
585 concentrations in the forest were underestimated by the model with the variable coefficients.
586 These results improved when the concentrations of ^{210}Pb (xs) of the ≤ 2 μm size fraction were
587 simulated, rather than that of the bulk soil, as a portion of the ^{210}Pb (xs) was adsorbed on the
588 organic particles > 2 μm at the soil surface.
589 The isotopes ^{137}Cs and ^{210}Pb (xs) are only relevant to trace the transfer of particles in the A
590 horizon over short periods of time (several tens of years). Therefore, the estimated velocities may
591 not be directly extrapolated to the entire soil profile. To explore the kinetics of vertical matter

592 transfers in deeper horizons, other tracers with a stronger affinity for clay and longer half-lives
593 (e.g., ^{241}Am or meteoric ^{10}Be) could be measured.
594
595 **Acknowledgements:**
596 This research was conducted in the framework of the Agriped project (ANR-10-BLANC-605),
597 which is supported by the French National Research Agency (ANR), and M. Jagercikova, who
598 received a PhD grant from the French National Institute for Agricultural Research (INRA).
599 The authors are grateful to Dr. Frédéric Golay, Dr. Cédric Galusinski and Dr. Gloria Faccanoni
600 for their suggestions regarding numerical modeling; to Monique Mayor and Fréderic Haurine for
601 their contributions to the sample preparations; to Patrick Signoret for the carbon analyses; to Dr.
602 Bruno Mary, Dr. David Montagne and Nicolas Brunet for providing the soil bulk density data; to
603 the Agriped team for contributing to the sampling; to INRA of Mons en Chaussée, Grignon and
604 Arvalis for providing access to their long-term experimental site and its associated data; and to
605 Meteo France for providing climatic data from the Safran Grid for the studied sites.
606
607 **References**
608 Anderson, J. M., 1988. Invertebrate-mediated transport processes in soils. Agric. Ecosyst.
609 Environ. 24 (1), 5-19.
610 Antoine, P., Catt, J., Lautridou, J. P., Sommé, J., 2003. The loess and coversands of northern
611 France and southern England. J. Quat. Sci. 18 (3- 4), 309-318.
612 Barnett, C. M., Bengough, A. G., McKenzie, B. M., 2009. Quantitative image analysis of
613 earthworm-mediated soil displacement. Biology and Fertility of Soils, 45(8), 821-828.

614 Bieri, M., Cuendet, G., 1989. Die Regenwürmer, eine wichtige Komponente von Ökosystemen.
615 Schweiz. Landw. Fo, 28 (2) 81-96.
616 Bockheim, J., Gennadiyev, A., 2000. The role of soil-forming processes in the definition of taxa
617 in Soil Taxonomy and the World Soil Reference Base. Geoderma 95 (1-2), 53–72.
618 Bossew, P., Kirchner, G., 2004. Modelling the vertical distribution of radionuclides in soil. Part
619 1: the convection-dispersion equation revisited. J. Environ. Radioact. 73 (2), 127–150.
620 Bouché, M. B., 1981. Contribution des lombriciens aux migrations d'éléments dans les sols
621 tempérés. Colloques Internationaux du Centre National de la Recherche Scientifique, No.
622 303, pp. 145-53.
623 Bouché, M.B., 1982. Ecosystème prairial. 4.3 Un exemple d'activité animale: le rôle des
624 lombriciens. Acta Oecol. Oecol. Gen. 3, 127–154.
625 Boudreau, B. P., 1986. Mathematics of tracer mixing in sediments; I, Spatially-dependent,
626 diffusive mixing. Am. J. Sci., 286 (3), 161-198.
627 Cambray, R. S., Playford, K., Lewis, G., Carpenter, R., 1989. Radioactive fallout in air and rain:
628 results to the end of 1988. Environmental and Medical Sciences Division, United
629 Kingdom Atomic Energy Authority.
630 Cerdan, O., Govers, G., Le Bissonnais, Y., Van Oost, K., Poesen, J., Saby, N., Gobin, A., Vacca,
631 A., Quinton, J., Auerswald, K., Klik, A., Kwaad, F.J.P.M., Raclot, D., Ionita, I., Rejman,
632 J., Rousseva, S., Muxart, T., Roxo, M.J., Dostal, T., 2010. Rates and spatial variations of
633 soil erosion in Europe: A study based on erosion plot data. Geomorphology 122 (1), 167-
634 177.
635 Chenu, C., Le Bissonnais, Y., Arrouays, D., 2000. Organic matter influence on clay wettability
636 and soil aggregate stability. Soil Sci. Soc. Am. J. 64 (4), 1479-1486.

637 Cornu, S., Quénard, L., Cousin, I., Samouëlian, A., 2014. Experimental approach of lessivage:
638 quantification and mechanisms. Geoderma 213, 357-370.
639 Cremers, A., Elsen, A., Depreter, P., Maes, A., 1988. Quantitative-analysis of radiocesium
640 retention in soils. Nature 335 (6187), 247–249.
641 Darwin, C., 1881. The formation of vegetable mould through the action of worms, with
642 observations on their habits. John Murray, London. 326 pp.
643 Dexter, A.R., 1993. Heterogeneity of unstaturated, gravitional flow of water through beds of
644 large particles. Water Resour. Res. 29 (6), 1859-1862.
645 Dimassi, B., Cohan, J. P., Labreuche, J., Mary, B., 2013. Changes in soil carbon and nitrogen
646 following tillage conversion in a long-term experiment in Northern France. Agric.,
647 Ecosyst. Environ. 169, 12-20.
648 Dörr, H., Münnich, K., 1989. Downward movement of soil organic-matter and its influence on
649 trace-element transport (Pb-210, Cs-137) in the soil. Radiocarbon 31 (3), 655–663, 13th
650 International Radiocarbon conf, Dubrovnik, Yugoslavia, Jun 20- 25, 1988.
651 Edwards, C. A., Lofty, J. R., 1977. Biology of Earthworms, 2nd edn. Chapman and Hall,
652 London.
653 Elzein, A., Balesdent, J., 1995. Mechanistic simulation of vertical distribution of carbon
654 concentrations and residence times in soils. Soil Sci. Soc. Am. J. 59 (5), 1328–1335.
655 Evrard, O., Vandaele, K., Bielders, C.L., van Wesemael, B., 2008. Seasonal evolution of runoff
656 generation on agricultural land in the Belgian loess belt and implications for muddy flood
657 triggering. Earth Surf. Process. Landforms 33 (8), 1285-1301.
658 Evrard, O., Némery, J., Gratiot, N., Duvert, C., Ayrault, S., Lefèvre, I., Poulenard, J., Prat, C.,
659 Bonté, P., Esteves, M., 2010. Sediment dynamics during the rainy season in tropical

highland catchments of central Mexico using fallout radionuclides. Geomorphology 124, 42-54.

Evrard, O., Van Beek, P., Gateuille, D., Pont, V., Lefèvre, I., Lansard, B., Bonté, P., 2012. Evidence of the radioactive fallout in France due to the Fukushima nuclear accident. J. Environ. Radioact. 114, 54-60.

Fedoroff, N., 1997. Clay illuviation in Red Mediterranean soils. Catena, 28, 171-189.

Finke, P. A., 2012. Modeling the genesis of Luvisols as a function of topographic position in loess parent material. Quat. Int. 265, 3-17.

Finke, P. A., Hutson, J. L., 2008. Modelling soil genesis in calcareous loess. Geoderma 145 (3), 462-479.

Gobat, J. M., Aragno, M., Matthey, W., 2004. The living soil: fundamentals of soil science and soil biology. Science Publishers.

He, Q., Walling, D., 1997. The distribution of fallout Cs-137 and Pb-210 in undisturbed and cultivated soils. App. Radiat. Isot. 48 (5), 677-690.

Hoogerkamp, M., Rogaar, H., Eijsackers, H. P., 1983. Effect of earthworms on grassland on recently reclaimed polder soils in the Netherlands. In Earthworm ecology (pp. 85-105). Springer Netherlands.

Jacobsen, O.H., Moldrup, P., Larson, C., Konnerup, L., Peteren, L.W., 1997. Particle transport in macropores of undisturbed soil columns. J. Hydrol. 196, 185–203.

Jamagne, M., 1973. Contribution à l'étude pédologique des formations loessiques du Nord de la France. Thèse de la faculté des sciences agronomiques de l'état, Gembloux Belgique 445 p.

682 Jamagne, M., 1978. Soil-forming processes in a progressive evolutionary sequence on loessial
683 silty formation in a cold and humid temperate zone. Comptes Rendus Hebdomadaires des
684 Séances de l'Académie des Sciences, Paris, 286 (1), 25-27.
685 Jamagne, M., Pedro, G., 1981. Les phénomènes de migration et d'accumulation de particules au
686 cours de la pédogenèse sur les formations limoneuses du Nord de la France. Essai de
687 caractérisation du processus de "lessivage". CRAS 292, 1329-1332.
688 James, S. W., 1991. Soil, nitrogen, phosphorus, and organic matter processing by earthworms in
689 tall grass prairie. Ecology 2101-2109.
690 Jarvis, N. J., Taylor, A., Larsbo, M., Etana, A., Rosen, K., 2010. Modelling the effects of
691 bioturbation on the re-distribution of 137Cs in an undisturbed grassland soil. Eur. J. Soil
692 Sci. 61 (1), 24–34.
693 Jenny, H., 1941. Factors of soil formation. McGraw-Hill Book Company New York.
694 Jones, A., Montanarella, L., Jones, R, 2005. Soil atlas of Europe. European Commission.
695 Kjaergaard, C., De Jonge, L. W., Moldrup, P., Schjønning, P., 2004. Water-Dispersible Colloids.
696 Vadose Zone J., 3(2), 403-412.
697 Khan, M.S.H., Parkash, B., Kumar, S., 2005. Soil-landform development of a part of the fold
698 belt along the eastern coast of Bangladesh. Geomorphology 71, 310-327.
699 Kollmannsperger, F., 1934. Die Oligochaeten des Bellinchengebietes, eine ökologische,
700 ethologische und tiergeographische Untersuchung (Doctoral dissertation, Druckerei W.
701 May).
702 Kretzschmar, A., 1982. Description des galeries de vers de terre et variation saisonnière des
703 réseaux (observations en conditions naturelles). Rev. Ecol. Biol. Sol 19 (4), 579-591.

704 Kühn, P., 2003. Morphology and late glacial/Holocene genesis of Luvisols in Mecklenburg-
705 Vorpommern (NE-Germany). Catena 54, 53-555.
706 Le Bissonnais, Y., Arrouays, D., 1997. Aggregate stability and assessment of soil crustability
707 and erodibility: II. Application to humic loamy soils with various organic carbon
708 contents. Eur. J. Soil Sci. 48 (1), 39-48.
709 Lee, K. E., 1985. Earthworms, Their Ecology and Relationships with Soils and Land Use.
710 Academic Press, Sydney.
711 Majdalani, S., Michel, E., Di Pietro, L., Angulo-Jaramillo, R., Rousseau, M., 2007. Mobilization
712 and preferential transport of soil particles during infiltration: A core-scale modeling
713 approach. Water Resour. Res. 43 (5).
714 Matisoff, G., Ketterer, M. E., Rosen, K., Mietelski, J. W., Vitko, L. F., Persson, H., Lokas, E.,
715 2011. Downward migration of Chernobyl-derived radionuclides in soils in Poland and
716 Sweden. Appl. Geochem. 26 (1), 105–115.
717 Matthey, W., Zettel, J., Bieri, M., 1990. Invertébrés bioindicateurs de la qualité des sols
718 agricoles, Wirbellose Bodentiere als Bioindikatoren für die Qualität von
719 Landwirtschaftsböden. Nationales Forschungsprogramm 'Boden' (NFP 22), Bericht Nr.
720 56, Liebefeld-Bern.
721 Montagne, D., Cousin, I., Josière, O., Cornu, S., 2013. Agricultural drainage-induced Albeluvisol
722 evolution: A source of deterministic chaos. Geoderma 193, 109-116.
723 Müller-Lemans, H., van Dorp, F., 1996. Bioturbation as a mechanism for radionuclide transport
724 in soil: Relevance of earthworms. J. Environ. Radioact. 31 (1), 7–20.
725 Munsell, A. H., 2000. Munsell soil color charts. Munsell Color.

726 Persson, T., Lenoir, L., Taylor, A., 2007. Bioturbation in different ecosystems at Forsmark and
727 Oskarhamn. SKB Rapport R-06-123. Stockholm Sweden.
728 Poesen, J. W., Verstraeten, G., Soenens, R., Seynaeve, L., 2001. Soil losses due to harvesting of
729 chicory roots and sugar beet: an underrated geomorphic process? Catena 43 (1), 35-47.
730 Preiss, N., Mélières, M. A., Pourchet, M., 1996. A compilation of data on lead 210 concentration
731 in surface air and fluxes at the air-surface and water-sediment interfaces. J. Geophy. Res.
732 101(D22), 28847-28862.
733 Quénard, L., Samouelian, A., Laroche, B., Cornu, S., 2011. Lessivage as a major process of soil
734 formation: A revisitation of existing data. Geoderma 167-168, 135–147.
735 Reynolds, J. W., 1970. The relationship of earthworm (Oligochaeta:Lumbricidae
736 and Medascolecidae) distribution and biomass to soil type in forest and grassland habitats
737 at Oak Ridge National Laboratory. Assoc. Southeast Biology Bulletin, vol. 17, 60 pp.
738 Rodriguez, M. D., 2006. The bioturbation transport of chemicals in surface soils (Doctoral
739 dissertation, Faculty of the Louisiana State University and Agricultural and Mechanical
740 College.
741 Rosén, K., Öborn, I., Lönsjö, H., 1999. Migration of radiocaesium in Swedish soil profiles after
742 the Chernobyl accident, 1987–1995. J. Environ. Radioact. 46 (1), 45-66.
743 Roussel-Debel, S., Renaud, P., Metivier, J. M., 2007. ^{137}Cs in French soils: Deposition patterns
744 and 15-year evolution. Sci. Total Environ. 374 (2), 388-398.
745 Sawhney, B., 1972. Selective sorption and fixation of cations by clay minerals: a review. Clays
746 Clay Miner. 20, 93–100.
747 Schiffers, K., Teal, L. R., Travis, J. M. J., Solan, M., 2011. An open source simulation model
748 for soil and sediment bioturbation. PloS ONE 6 (12), e28028.

749 Schimmack,W., Feria Marquez, F., 2006. Migration of fallout radiocaesium in a grassland soil
750 from 1986 to 2001 - Part II: Evaluation of the activity-depth profiles by transport models.
751 Sci. Total Environ. 368 (2-3), 863–874.
752 Schmidt, M. W. I., Rumpel, C., Kögel- Knabner, I., 1999. Evaluation of an ultrasonic dispersion
753 procedure to isolate primary organomineral complexes from soils. Eu. J. Soil Sci. 50 (1),
754 87-94.
755 Schuller, P., Bunzl, K., Voigt, G., Ellies, A., Castillo, A., 2004. Global fallout Cs-137
756 accumulation and vertical migration in selected soils from South Patagonia. J. Environ.
757 Radioact. 71 (1), 43–60.
758 Schuller, P., Ellies, A., Kirchner, G., 1997. Vertical migration of fallout Cs-137 in agricultural
759 soils from Southern Chile. Sci. Total Environ. 193 (3), 197–205.
760 Smith, J., Elder, D., 1999. A comparison of models for characterizing the distribution of
761 radionuclides with depth in soils. Eur. J. Soil Sci. 50 (2), 295–307.
762 Stöckli, A., 1928. Studien über den Einfluss des Regenwurmes auf die Beschaffenheit des
763 Bodens. Landwirtschuftliches Juhrbuch der Schweiz, 42 (l), 1-121 (Diss ETH 492,
764 Zurich).
765 Syers, J. K., Sharpley, A. N., Keeney, D. R., 1979. Cycling of nitrogen by surface-casting
766 earthworms in a pasture ecosystem. Soil Biol. Biochem., 11(2), 181-185.
767 Tamura, T., Jacobs, D., 1960. Structural implications in cesium sorption. Health Phys. 2 (4),
768 391–398.
769 Ullrich, A., Volk, M., 2009. Application of the Soil and Water Assessment Tool (SWAT) to
770 predict the impact of alternative management practices on water quality and quantity.
771 Agric. Water Manag. 96 (8), 1207-1217.

772 Van Breemen, N., Buuerman, P., 2002. Soil formation. Springer.
773 Van Oost, K., Cerdan, O., Quine, T. A., 2009. Accelerated sediment fluxes by water and tillage
774 erosion on European agricultural land. Earth Surf. Process. Landforms 34 (12), 1625-
775 1634.
776 Wilkinson, M. T., Richards, P. J., Humphreys, G. S., 2009. Breaking ground: Pedological,
777 geological, and ecological implications of soil bioturbation. Earth-Science Reviews 97
778 (1-4), 257–272.
779
780 Figure 1: Observed and modeled distributions of ^{137}Cs under three land uses at each of the
781 studied sites. The modeling duration for the Mons and Feucherolles sites was from 1954 to 2011
782 (57 years) and for the Boigneville site from 1954 to 2012 (58 years). In the legend: cDiff -
783 constant diffusion, vDiff - variable diffusion, cVel - constant velocity, and vVel - variable
784 velocity. No diffusion coefficient was used to simulate the tilled plots.
785
786 Figure 2: Organic carbon content and the index of clay migration according to pH (IMCpH). CT
787 - conventional tillage, RT - reduced tillage, NT - no tillage, MI - manure input, G - grassland,
788 and F - forest.
789
790 Figure 3: Comparison of the mean diffusion coefficients calculated for the upper 30 cm, the
791 mean convection velocities calculated for the upper 40 cm and the annual erosion rates with the
792 different model settings. CT - conventional tillage; RT - reduced tillage; NT - no tillage; MI -
793 manure input, G - grassland, F – forest, nDiff - no diffusion, cDiff - constant diffusion, vDiff -

794 variable diffusion (no diffusion for tilled plots), cVel - constant velocity, and vVel - variable
795 velocity.

796

797 Figure 4: Comparison of ^{210}Pb (xs) in the fraction coarser than 2 µm and organic carbon in the
798 fraction coarser than 2 µm in the surface samples.

799 Figure 5: Modeling results of the ^{210}Pb (xs) distributions in the bulk soil samples (left and middle
800 figures) and in the 0-2 µm fraction for the forest (figure at right). Modeling duration was from
801 1700 to 2011 (311 years). cDiff - constant diffusion, vDiff - variable diffusion, cVel - constant
802 velocity, vVel - variable velocity.

803 Table 1: General description of the studied sites.

804 Table 2: Synthetic soil description of the different plots and sites.

805 Table 3: Pedologic characteristics of the studied sites.

806 Table 4: Modeling setup (with/without erosion and diffusion) and initial parameters for fallout
807 due to the Chernobyl accident in 1986 (a_{Ch}), tillage depth (T_D) and mixing ratio induced by the
808 tillage (M_R). Models with variable convection velocities simulate the change in the velocity as
809 segment-lines, with fixed endpoint depths specifically determined for each site according to its
810 pedologic characteristics.

811 Table 5: ^{137}Cs and ^{210}Pb (xs) inventories on the sampling date.

812 Table 6: ^{137}Cs and ^{210}Pb (xs) activities measured by gamma spectroscopy in the ≤ 2 µm size
813 fraction. The ratio of activities in the ≤ 2 µm fraction to the total activities in the bulk soil sample
814 is expressed as a %. < DL – below the detection limit

Table 7: Modeling results of the ^{137}Cs vertical distribution in the studied soils. The modeling was performed either without or with diffusion (constant or exponentially decreasing) and with constant convection velocity. D_0 - diffusion coefficient at the surface, D_s - diffusion coefficient, b - parameter of exponentially decreasing diffusion, v_s - convection velocity coefficient, E - erosion parameter, EF - modeling efficiency, RSS - residual sum of squares, SD - standard deviation, ± uncertainty, CT - conventional tillage, RT - reduced tillage, NT - no tillage and MI - manure input.

Table 8: Modeling results of the ^{137}Cs vertical distribution in studied soils. The modeling was performed either without or with diffusion (exponentially decreasing) and with variable convection velocity. D_0 - diffusion coefficient at the surface, D_s - diffusion coefficient, b - parameter of exponentially decreasing diffusion, v_0 - convection velocity at the surface, v_1 - convection velocity at a given endpoint (depth z in parenthesis), v_2 - convection velocity at a given endpoint (depth z in parenthesis), v_s - convection velocity coefficient, E - erosion parameter, EF - modeling efficiency, RSS - residual sum of squares, SD - standard-deviation, ± uncertainty, CT - conventional tillage, RT - reduced tillage, NT - no tillage and MI - manure input.

Table 9: Bioturbation rates and surface cast rates generated by earthworms in the soil under deciduous forests and grasslands in a humid temperate climate.

Table 1: General description of the studied sites.

Site	Mons	Feucherolles	Boigneville
Experiment name	Essay system – ORE-ACBB[a] Mons	ORE-PRO[b]-Qualiagro	Wheat monoculture
Managing institution	INRA	INRA	Arvalis (Plant institute)
Geographic coordinates	49°52'01"N - 3°01'53" E	48°53'49"N - 1°58'19"E	2°22'58''E - 48°19'30''N
Elevation	88 m	120 m	116 m
Mean annual rainfall	680 mm	660 mm	630 mm
Mean annual temperature	11 °C	11.2 °C	10.4 °C
Considered landuses and farming practices	- Conventional tillage - Reduced tillage (since 2000) - Grassland (since 1939)	- Conventional tillage without manure or fertilizers (since 1998) - Conventional tillage with manure (since 1998) - Oak forest (since 1815 at least according to Cassini maps)	- Conventional tillage - Reduced tillage (since 1970) - No tillage (since 1970)
Crop rotation	Wheat - corn - sugarbeet	Corn - wheat	Wheat
Liming	Not since 1986 under cultivation and 1939 for pasture	Not since 1998 under cultivation	Not since 1970
Maximal distance among plots	2 km	2 km	A few tens of meters
Sampling date	March 2011	April 2011	March 2012

[a]- Observatory for Environmental Research on agrosystems, biogeochemical cycles and biodiversity

[b]- Observatory for Environmental Research for organic residual products

Table 2: Synthetic soil description of the different plots and sites.

Sites	Plots	Horizon A	E	Degraded Bt	Bt	C/Bt	C	II
Mons	**Conventional tillage**	Silt-loam, 10YR4/4 [a]: 0-28 cm: tillage horizon, crumbly, no earthworms; 28-38 cm: base of the ancient tillage, polyhedral, few earthworms.	none	none	38-130 cm, silty clay-loam, prismatic, 10YR4/4[a] with 7.5YR4/4 coatings, few earthworms.	130-150 cm, silt-loam, continuous, 10YR5/6, few earthworms.	> 150 cm, same characteristics than C/Bt no earthworm	none
	Reduce tillage[b]	0-10 cm, tillage; 10-15 cm, compact and lamellar	idem					
	Pasture[b]	richer in organic matter and earthworm activity, exhibiting darker colours (10 YR 3/2) and frequent earthworm casts						
Feucherolles	**Conventional tillage and Tillage and manure**	0-25(27) cm: tillage horizon, silt loam, crumbly to polyhedrous, 10YR4/4[a]; 25(27)-32(35) cm: base of the former tillage, poorly polyhedrous.	32(35)- 45(50) cm, silt loam, poorly polyhedrous, 10YR4/6[a]	45(50)-75(80) cm: silty clay loam, prismatic, 7.5YR4/6[a] with 10YR4/6 tongues	75(80)-95(100) cm: silty clay loam, 10YR5/6[a] with 7.5YR4/6 coatings	none	95(100)-160 cm, silt loam, 10 YR 5/6[a], water-logged at its base during sampling; 160-168(172) cm, carbonated Ck	> 168 (172) cm, clays with gritstone gravels
	Oak forest[b]	0-10(15) cm, crumbly silt loam, 10 YR 3/3[a]	10(15)-40 cm, 10 YR 4/4	40 and 122 cm, less degraded, more variable laterally		idem	idem	idem
Boigneville	**Conventional tillage**	0-20(25) cm: tillage horizon, silt loam, crumbly, 10YR4/4 [a]; 20(25)-35 cm, former tillage, compact, more clayey, 10YR3/3.5	none	none	34(50)-73(80) cm, silty clay loam to silty clay, prismatic, 10YR4/4[a] with 10YR3/4 coatings	none	none	>73(80) cm, transition to another parent material
	Reduced tillage[b]	0 to 5 (10) cm: tillage horizon, 10YR 3.5/2; 5(10)-25(30) cm: former tillage, silty clay loam texture, lamellar structure, 10YR 4/3.5.	earthworms were abundant down to 45 cm depth			idem	idem	idem
	No tillage[b]	0-10 cm, 10YR3/2, crumbly 10-25 cm, 10Y 4/3, polyhedral	idem			idem	idem	idem

[a] according to the Munsell Soil Color Chart, 2000

[b] only changes compared to the reference tilled profile of the same site were described

Table 3: Pedologic characteristics of the studied sites.

Horizon	Depths	Particle size in g kg^{-1}					Organic carbon	pH	CEC	$CaCO_3$ total	Bulk density
	cm	0-2 µm	2-20 µm	20-50 µm	50-200 µm	200-2000 µm	g kg^{-1}	(H_2O)	cmol(+) kg^{-1}	g kg^{-1}	g cm^{-3}
Mons: Conventional Tillage											
Ap	0-27	192	315	435	46	12	11.8	7.84	11.9	<1	1.40
A2	27-37	219	315	414	44	8	9.0	8.05	12.5	<1	1.43
Bt1-Bt3	37-125	287	279	395	37	3	2.8	8.09	15.8	<1	1.50
C/Bt	125-145	219	227	530	23	2	1.7	8.15	12.9	<1	1.42
C	145-155	184	224	575	16	1	1.3	8.07	11.0	<1	1.36
Mons: Reduced Tillage											
Ap	0-10	212	301	428	51	9	12.9	7.34	11.5	<1	1.34
A2	10-15	207	308	431	48	7	10.2	7.76	11.3	<1	1.49
A3	15-42	206	316	424	45	8	9.4	8.00	11.8	<1	1.50
Bt1-Bt3	42-125	260	260	436	42	2	2.6	8.04	14.7	<1	1.48
C/Bt	125-145	209	226	544	20	2	1.5	7.87	12.0	<1	1.41
C	145-155	192	237	558	12	1	1.1	8.00	10.7	<1	1.37
Mons: Grassland											
A1	0-10	202	303	438	46	11	28.6	6.07	14.1	<1	1.20
A2	10-40	201	307	432	49	12	14.5	6.68	13.7	<1	1.39
Bt1-Bt3	40-102	277	300	376	42	4	3.8	7.27	16.4	<1	1.50
C/Bt	102-142	244	221	493	40	3	1.7	7.51	15.5	<1	1.45
C	142-162	190	255	537	17	2	1.3	7.56	11.9	<1	1.38
Feucherolles: Conventional tillage											
Ap	0-25	142	296	495	54	13	9.4	6.59	7.7	<1	1.36
A2	25-31	144	300	483	61	13	9.5	6.61	7.9	<1	1.41
E	31-50	211	295	430	46	19	3.8	6.99	9.4	<1	1.48
Btgd	50-75	298	268	384	38	12	2.6	7.34	14.3	<1	1.53
Bt2	75-95	331	208	437	22	3	2.1	7.43	18.4	<1	1.51
C/Bt	95-145	244	236	492	26	2	1.3	7.63	14.5	<1	1.51

C	145-165	207	270	493	26	4	1.3	7.66	14.2	<1	1.54

Horizon	Depths	Particle size in g kg^{-1}					Organic carbon	pH	CEC	$CaCO_3$ total	Bulk density
	cm	0-2 µm	2-20 µm	20-50 µm	50-200 µm	200-2000 µm	g kg^{-1}	(H_2O)	cmol(+) kg^{-1}	g kg^{-1}	g cm^{-3}
Feucherolles: Conventional tillage and manure											
Ap	0-25	144	296	489	55	16	14.0	7.27	9.7	<1	1.33
A2	25-33	145	292	491	59	15	10.0	7.38	8.6	<1	1.45
E	33-50	192	290	455	47	17	5.0	7.45	8.9	<1	1.57
Btgd	50-80	305	253	400	31	11	2.7	7.56	14.8	<1	1.59
Bt2	80-100	309	201	469	20	3	1.9	7.49	17.3	<1	1.52
C	100-160	225	260	459	27	15	1.7	7.49	14.8	22.25	1.52
Ck	160-170	194	255	343	44	21	0.9	8.53	14.0	140	1.65
Feucherolles: Oak forest											
A	0-10	176	284	463	64	13	30.5	5.55	11.4	<1	1.00
E	10-40	167	288	463	66	17	10.9	5.12	6.8	<1	1.28
Bt1-Bt2	40-95	228	281	420	55	16	3.2	5.72	9.1	<1	1.47
Bt3	95-125	305	196	465	28	6	1.9	6.23	17.1	<1	1.55
C	125-147	243	248	484	24	2	2.0	6.84	14.5	<1	1.52
Ck	147-157	137	240	457	19	2	0.9	8.55	11.3	143	1.49
Boigneville: Conventional Tillage											
Ap	0-24	256	306	357	63	19	12.1	6.91	14.9	<1	1.35
E	24-35	263	305	354	62	17	9.1	7.28	15.6	<1	1.45
Bt1	35-80	375	286	300	33	6	3.9	7.85	21.6	3.07	1.50
II	80-100	177	188	118	38	5	2.5	8.87	11.0	467.5	1.47
Boigneville: Reduced Tillage											
Ap	0-5	256	293	372	60	19	24.9	6.09	13.2	<1	1.26
Ap2	5-31	264	298	358	62	18	11.8	6.71	14.5	<1	1.41
Bt1-Bt2	31-74	371	280	299	42	8	4.6	7.75	21.1	1.68	1.51
II	74-95	176	271	150	57	6	4.4	8.71	16.2	334	1.47

Horizon	Depths	Particle size in g kg^{-1}					Organic carbon	pH	CEC	$CaCO_3$ total	Bulk density
	cm	0-2 µm	2-20 µm	20-50 µm	50-200 µm	200-2000 µm	g kg^{-1}	(H_2O)	cmol(+) kg^{-1}	g kg^{-1}	g cm^{-3}
Boigneville: **No-tillage**											
A	0-10	238	302	364	71	24	24.4	5.69	12.1	<1	1.24
A2	10-25	249	299	359	70	24	10.4	6.87	14.1	<1	1.53
E	25-45	328	295	317	47	13	6.0	7.43	17.1	<1	1.49
Bt	45-80	377	288	293	34	8	3.6	7.77	20.9	2	1.50
II	80-100	212	227	87	42	5	3.2	8.84	12.3	421.5	1.47

Table 4: Modeling setup (with/without erosion and diffusion) and initial parameters for fallout due to the Chernobyl accident in 1986 (a_{Ch}), tillage depth (T_D) and mixing ratio induced by the tillage (M_R). Models with variable convection velocities simulate the change in the velocity as segment-lines, with fixed endpoint depths specifically determined for each site according to its pedologic characteristics.

Site	**Erosion**	**Diffusion**	a_{Ch} **Bq m^{-2}**	T_D **cm**	M_R	**Fixed end-point depth cm**
Mons: Conventional tillage	Yes	No	661	28	0.85	0 and 20
Mons: Reduced tillage	Yes	No	661	28 (1954-1999) 10 (2000-2011)	0.85 (1954-1999) 0.30 (2000-2011)	0 and 20 and 40
Mons: Grassland	No	Yes	661	—	—	0 and 40 and 100
Feucherolles: Conventional tillage	Yes	No	413	25	0.85	0 and 20 and 80
Feucherolles: Manure	Yes	No	413	25	0.85	0 and 40
Feucherolles : Oak forest	No	Yes	413	—	—	0 and 20 and 40
Boigneville: Conventional tillage	Yes	No	499	25 (1954-1999) 20 (2000-2012)	0.85 (1954-1999) 0.85 (2000-2012)	0 and 26 and 40
Boigneville: Reduced tillage	Yes	No	499	23 (1954-1969) 10 (1970-1999) 5 (2000-2012)	0.85 (1954-1969) 0.30 (1970-1999) 0.30 (2000-2012)	0 and 14 and 30
Boigneville: No tillage	Yes	Yes (since 1970)	499	23 (1954-1969) — (1970-2012)	0.85 (1954-1969) — (1970-2012)	0 and 14 and 30

Table 5: ^{137}Cs and ^{210}Pb (xs) inventories on the sampling date.

Site	**Plot**	**^{137}Cs inventory Bq m^{-2}**	**Error Bq m^{-2}**	**^{210}Pb (xs) inventory Bq m^{-2}**	**Error Bq m^{-2}**
Mons	Conventional tillage	1419	129		
	Reduced tillage	1505	155	938	504
	Grassland	2075	184	1548	1377
Feuchehrolles	Conventional tillage	1451	167		
	Tillage and manure	1556	111	1478	747
	Oak forest	1878	217	1921	1959
Boigneville	Conventional tillage	1736	182		
	Reduced tillage	1518	138	1067	621
	No-tillage	1479	183	813	735

Table 6: ^{137}Cs and ^{210}Pb (xs) activities measured by gamma spectroscopy in the 0-2 µm size fraction. The ratio of activities in the 0-2 µm fraction to the total activities in the bulk soil sample is expressed as a %. < DL – below the detection limit

Depths cm	^{137}Cs 0-2 µm Bq kg^{-1}	Error Bq kg^{-1}	^{210}Pb (xs) 0-2 µm Bq kg^{-1}	Error Bq kg^{-1}	Clay (0-2 µm) g kg^{-1}	^{137}Cs % 0-2 µm in bulk %	Error %	^{210}Pb (xs) % 0-2 µm in bulk %	Error %
Mons: Reduced Tillage									
5-10	10.3	0.7	38	6	208	72	13	135	70
12-15	14.2	0.8	26	6	206	93	15	> 100	—
25-30	14.7	0.6	32	4	208	103	16	> 100	—
Mons: Conventional Tillage									
10-15	12.1	0.7	36	5	203	82	13	> 100	—
33-35	6.0	0.5	≤	9	234	91	18	< DL	—
Mons: Grassland									
0-2	18.5	0.8	45	5	201	88	12	54	15
2-4	18.3	0.8	30	5	205	86	12	62	24
18-20	18.4	0.5	29	3	199	91	11	117	59
45-50	1.2	0.5	≤	11	242	71	45	< DL	—
Feucherolles: Conventional Tillage									
10-15	20.7	0.7	39	4	142	86	11	> 100	—
27-29	20.3	0.5	38	3	145	88	11	> 100	—
Feucherolles: Manure									
10-15	22.1	0.6	43	4	145	102	14	148	90
27-29	21.3	0.8	33	5	146	93	11	116	63
33-35	12.7	0.5	24	4	149	96	17	> 100	—

Feucherolles: Oak forest									
0-2	41.5	1.3	92	8	185	99	12	52	11
2-4	41.6	1.2	83	7	180	97	11	87	23
16-18	36.3	1.0	15	5	170	92	10	> 100	—
40-45	≤	0.8	10	4	213	<DL	—	> 100	—
Boigneville: Conventional Tillage									
5-10	14.2	0.9	≤	13	260	92	16	< DL	—
31-33	9.8	0.9	≤	14	262	97	22	< DL	—
Boigneville: Reduced Tillage									
0-5	16.5	0.7	41	5	256	93	13	80	28
13-15	14.9	0.5	≤	6	270	106	13	< DL	—
Boigneville: No tillage									
0-2	19.1	0.8	54	6	235	106	16	63	22
2-4	19.2	0.8	38	5	229	91	13	55	24
18-20	11.9	0.6	≤	8	250	78	11	< DL	—

Table 7: Modeling results of the ^{137}Cs vertical distribution in the studied soils. The modeling was performed either without or with diffusion (constant or exponentially decreasing) and with constant convection velocity. D_0 - diffusion coefficient at the surface, D_s - diffusion coefficient, b - parameter of exponentially decreasing diffusion, v_s - convection velocity coefficient, E - erosion parameter, EF - modeling efficiency, RSS - residual sum of squares, SD - standard deviation, ± uncertainty, CT - conventional tillage, RT - reduced tillage, NT - no tillage and MI - manure input.

Site	D_0	**SD**	b	**SD**	**Mean** D_s	**SD**	v_s	**SD**	E	**SD**	EF	$RSS\ 10^{-6}$	**Annual erosion**			
	$cm^2\ yr^{-1}$	$cm^2\ yr^{-1}$			(0-30 cm) $cm^2\ yr^{-1}$	$cm^2\ yr^{-1}$	$cm\ yr^{-1}$	$cm\ yr^{-1}$	10^{-3} cm	10^{-3} cm			$mm\ yr^{-1}$	± $mm\ yr^{-1}$	$t\ ha^{-1}\ yr^{-1}$	± $t\ ha^{-1}\ yr^{-1}$
Without diffusion																
Mons: CT	—	—	—	—	—	—	0.14	0.005	14.06	0.65	0.99	4.7	0.70	0.16	9.80	2.43
Mons: RT	—	—	—	—	—	—	0.15	0.006	11.85	0.98	0.98	13.3	0.59	0.24	8.10	3.48
Feucherolles: CT	—	—	—	—	—	—	0.13	0.006	9.88	0.79	0.99	9.7	0.49	0.20	6.77	2.82
Feucherolles: CT + MI	—	—	—	—	—	—	0.23	0.005	6.45	0.84	0.98	13.6	0.32	0.21	4.23	2.82
Boigneville: CT	—	—	—	—	—	—	0.18	0.008	2.74	0.93	0.98	18.7	0.14	0.24	1.81	3.10
Boigneville: RT	—	—	—	—	—	—	0.09	0.003	5.00	0.59	0.97	11.2	0.25	0.15	2.73	1.66
Constant diffusion																
Boigneville: NT	0.13	0.08	—	—	—	—	0.08	0.01	7.35	2.34	0.80	79.0	0.37	0.59	4.41	7.09
Feucherolles: Oak forest	1.10	0.22	—	—	—	—	0.14	0.02	—	—	0.78	110.0	—	—	—	—
Mons: Grassland	2.55	0.27	—	—	—	—	0.29	0.02	—	—	0.96	31.7	—	—	—	—
Variable diffusion																
Boigneville: NT	0.001	0.001	1.00	1.32	3.33E-05	7.73E-05	0.07	0.003	3.36	0.74	0.95	8.2	0.17	0.19	2.02	2.26
Feucherolles: Oak forest	48.8	104.87	0.34	0.15	4.78	12.39	0.14	0.04	—	—	0.87	67.5	—	—	—	—
Mons: Grassland	5.42	1.81	0.04	0.01	3.16	1.92	0.26	0.02	—	—	0.97	19.6	—	—	—	—

Table 8: Modeling results of the ^{137}Cs vertical distribution in studied soils. The modeling was performed either without or with diffusion (exponentially decreasing) and with variable convection velocity. D_0 - diffusion coefficient at the surface, D_s - diffusion coefficient, b - parameter of exponentially decreasing diffusion, v_0 - convection velocity at the surface, v_1 - convection velocity at a given endpoint (depth z in parenthesis), v_2 - convection velocity at a given endpoint (depth z in parenthesis), v_s - convection velocity coefficient, E - erosion parameter, EF - modeling efficiency, RSS - residual sum of squares, SD - standard-deviation, ± uncertainty, CT - conventional tillage, RT - reduced tillage, NT - no tillage and MI - manure input.

Site	D_0	SD	b	SD	Mean D_s (0-30 cm)	SD	v_0 (z=0)	SD	v_1	SD	v_2	SD	Mean v_s (0-40 cm)	SD	E	SD	EF	$RSS\ 10^{-6}$	Annual erosion			
	$cm^2\ yr^{-1}$	$cm^2\ yr^{-1}$			$cm^2\ yr^{-1}$	$cm^2\ yr^{-1}$	$cm\ yr^{-1}$	$cm\ yr^{-1}$	$cm\ yr^{-1}$	$cm\ yr^{-1}$	$cm\ yr^{-1}$	$cm\ yr^{-1}$	$cm\ yr^{-1}$	$cm\ yr^{-1}$	10^{-3} cm	10^{-3} cm			$mm\ yr^{-1}$	± $mm\ yr^{-1}$	$t\ ha^{-1}\ yr^{-1}$	± $t\ ha^{-1}\ yr^{-1}$
Without diffusion																						
Mons: CT	—	—	—	—	—	—	0.03	0.15	0.14 (z=20)	0.006	—	—	0.11	0.16	14.02	0.68	0.99	4.39	0.70	0.17	9.80	2.54
Mons: RT	—	—	—	—	—	—	0.23	0.05	0.12 (z=20)	0.02	0.19 (z=40)	0.03	0.16	0.10	11.50	0.91	0.99	8.92	0.58	0.23	7.96	3.28
Feucherolles : CT	—	—	—	—	—	—	0.00	1.28	0.12 (z=20)	0.02	0.24 (z=80)	0.17	0.1	1.47	9.99	0.89	0.99	9.09	0.50	0.22	6.99	3.23
Feucherolles: CT + MI	—	—	—	—	—	—	0.09	0.05	—	—	0.29 (z=40)	0.02	0.19	0.07	6.94	0.65	0.99	6.66	0.35	0.16	4.86	2.36
Boigneville: CT	—	—	—	—	—	—	0.05	0.08	0.17 (z=26)	0.01	0.25 (z=40)	0.04	0.14	0.13	2.89	0.68	0.99	6.96	0.14	0.16	1.91	2.28
Boigneville: RT	—	—	—	—	—	—	0.1	0.02	0.09 (z=14)	0.01	0.09 (z=30)	0.01	0.09	0.04	4.75	0.63	0.97	9.51	0.24	0.16	2.59	1.76
Variable diffusion																						
Boigneville: NT	0.0003	0.002	0.46	74.3	2.17E-05	0.0038	0.06	0.07	0.05 (z=14)	0.03	0.08 (z=30)	0.02	0.06	0.12	2.47	3.82	0.99	2.90	0.12	0.93	1.48	11.47
Feucherolles: Oak forest	45.16	130.26	0.26	0.07	5.79	18.25	0.18	0.29	0.09 (z=20)	0.32	2.06 (z=40)	1.15	0.59	1.76	—	—	0.97	15.2	—	—	—	—
Mons: Grassland	3.68	2.04	0.08	0.10	1.39	2.63	0.18	0.08	0.71 (z=40)	0.56	0 (z=100)	3.07	0.44	0.64	—	—	0.98	18.3	—	—	—	—

Table 9: Bioturbation rates and surface cast rates generated by earthworms in the soil under deciduous forest and pasture for humid temperate climate.

Land use	References	Location	Earthworm type	Biomass g m^{-2}	Bioturbation t ha^{-1} yr^{-1}	Surface cast[c] t ha^{-1} yr^{-2}
Deciduous forest						
	Kollmannsperger (1934)	Germany	Lumbricidae			68
	Persson et al. (2007)	Sweden	Endogeic, epigeic	4-35	40-420	0.8-5
	Reynolds (1970)	Tennessee (USA)	Lumbricidae	1.3-14	2.6-28 [a]	
	Rodriguez (2006)	Germany	Lumbricidae			58
Grassland						
	Anderson (1988)	UK				40-50
	Bieri and Cuendet (1989) in Müller-Lemans and van Dorp, (1996)	Switzerland	Anecic 80%	270	432[b]	
	Bouché (1981) in Müller-Lemans and van Dorp, (1996)	France	Anecic 80%	121	193.6 [b]	60
	Bouché (1982)	France	Lumbricidae	165.4	330.8 [a]	7
	Darwin (1881)	UK				44.7
	Edwards and Lofty (1977) in Müller-Lemans and van Dorp, (1996)					91.4
	Gobat et al. (2004)	Switzerland				18-81
	Gobat et al. (2004)	UK				91
	Gobat et al. (2004)	Germany				19-40
	Hoogerkamp et al. (1983) in Müller-Lemans and van Dorp, (1996)	The Netherlands	Anecic 80%	250	400 [b]	
	James (1991)	Kansas (USA)	Diplocardia spp and Lumbricidae	1.44 ± 1.35 and 1.39 ± 2.23	5.7 ± 7.2 [a]	1.91
	James (1991)	Kansas (USA)	Diplocardia spp and Lumbricidae	0.95 ± 0.54 and 4.43 ± 3.6	10.8 ± 8.3 [a]	2.81
	Kretzschmar (1982) in Müller-Lemans and van Dorp, (1996)	France	Anecic 80%	200	320 [b]	29-134
	Lee (1985) in Müller-Lemans and van Dorp, (1996)	UK	Anecic 80%	149	238.4 [b]	
	Lee (1985) in Müller-Lemans and van Dorp, (1996)	France	Anecic 80%	165.4	264.6 [b]	70
	Lee (1985) in Müller-Lemans and van Dorp, (1996)	Germany	Anecic 80%	96.5	154.4 [b]	
	Matthey et al. (1990) in Müller-Lemans and van Dorp, (1996)	Switzerland	Anecic 80%	34-272	54.4-435.2 [b]	

Persson et al. (2007)	Sweden	Endogeic, epigeic	10-30	110-360	2-4
Reynolds (1970)	Tennessee (USA)	Lumbricidae	3.2-7.5	6.4-15[a]	
Stöckli (1928) in Müller-Lemans and van Dorp, (1996)	Switzerland				24.7-44.1
Stöckli (1928) in Müller-Lemans and van Dorp, (1996)	Switzerland				31.8-36
Syers et al. (1979)	New Zealand				2.5-3.3

[a] Bioturbation calculated after Bouché (1981): anecic earthworm biomass (g m^{-2}) x 200 (consumption of equivalent dry matter per year) = bioturbation rate (g m^{-2} yr^{-1})

[b] Bioturbation calculated after Bouché (1981) with hypothesis that anecic species represent in average 80 % of total biomass (Müller-Lemans and van Dorp, 1996)

[c] Bioturbation estimated on the base of the earthworm surface rejections (casts). Although classical (Gobat et al., 2004), this method only considers the surface rejections and thus underestimates bioturbation (Persson et al., 2007).

Figure 1

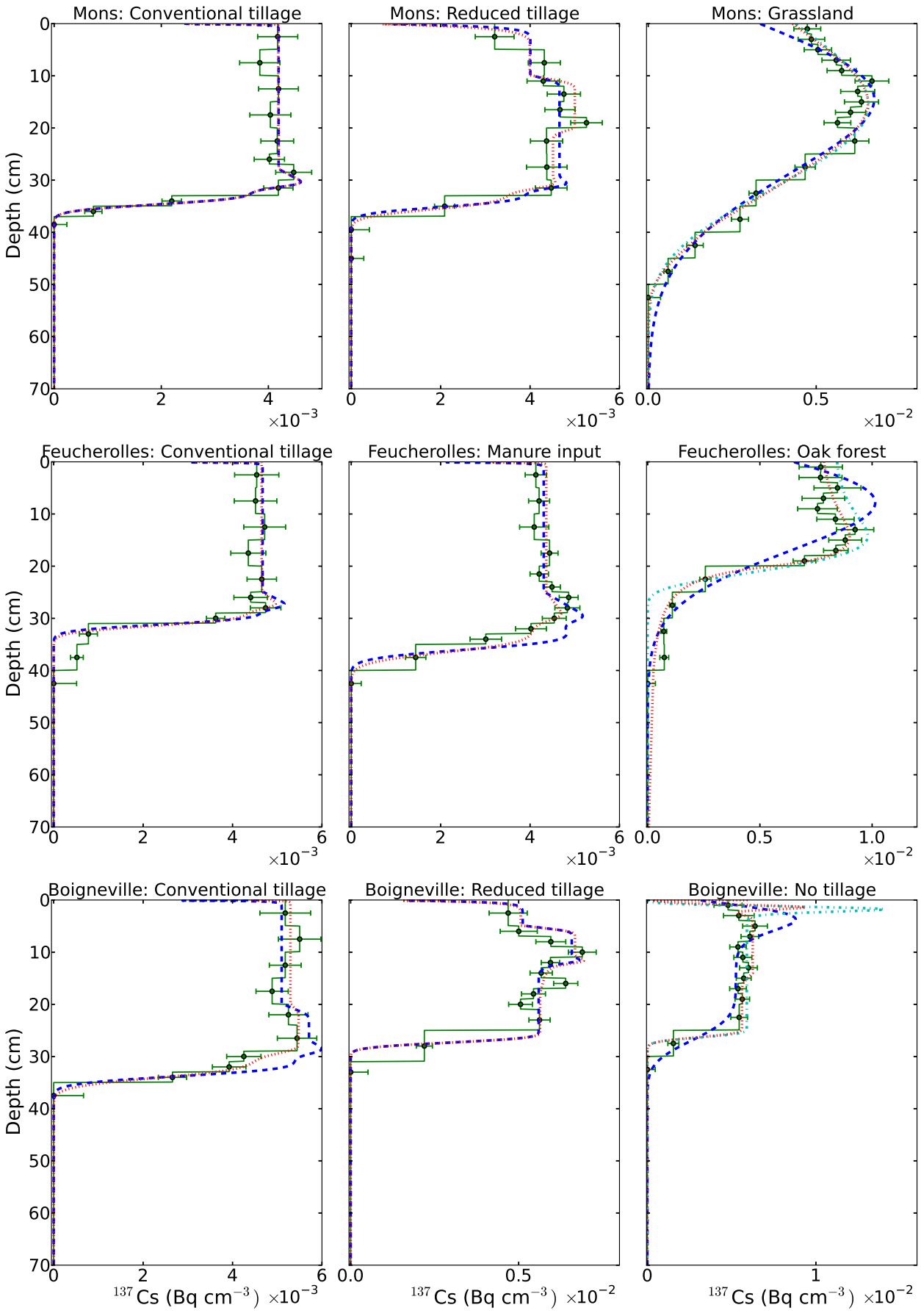
Mons: Conventional tillage
Mons: Reduced tillage
Mons: Grassland
Feucherolles: Conventional tillage
Feucherolles: Manure input
Feucherolles: Oak forest
Boigneville: Conventional tillage
Boigneville: Reduced tillage
Boigneville: No tillage
Depth (cm)
^{137}Cs (Bq cm^{-3}) ×10^{-3}
^{137}Cs (Bq cm^{-3}) ×10^{-2}
Data
Model cDiff_cVel
Model vDiff_cVel
Model vDiff_vVel

Figure 2

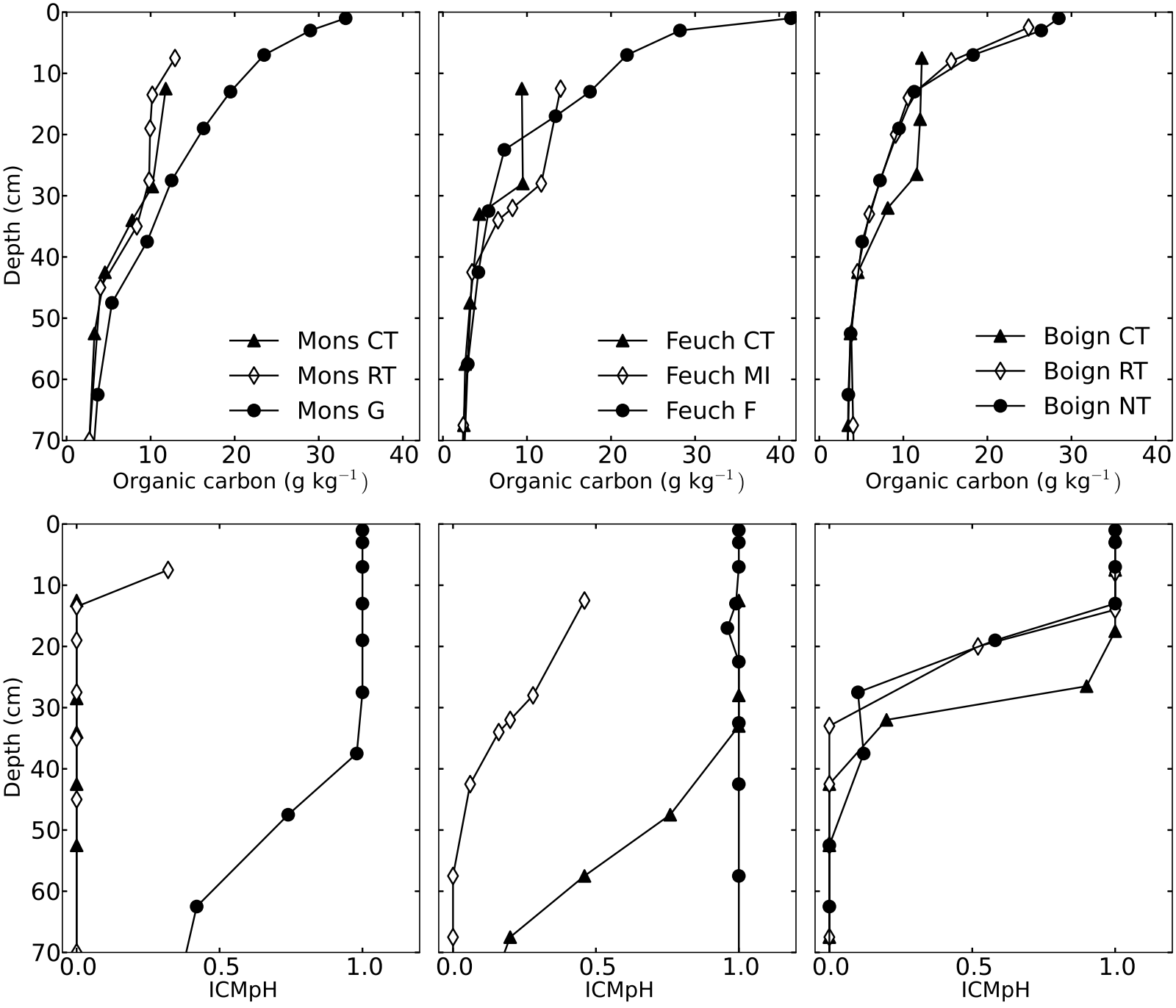
Depth (cm)
0
10
20
30
40
50
60
70
0
10
20
30
40
Organic carbon (g kg^{-1})
Mons CT
Mons RT
Mons G
Feuch CT
Feuch MI
Feuch F
Boign CT
Boign RT
Boign NT
0.0
0.5
1.0
ICMpH

Figure 3

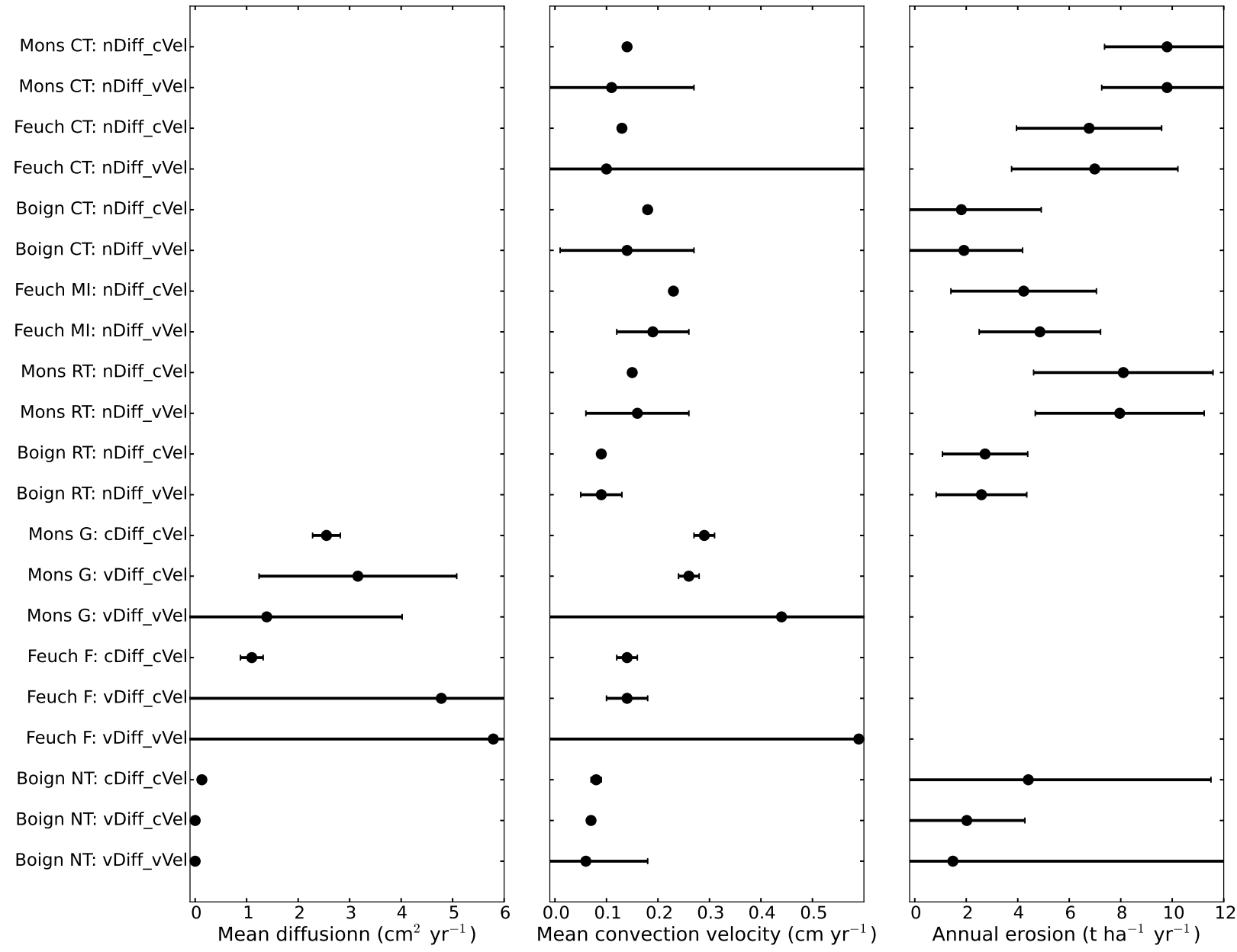
Mons CT: nDiff_cVel
Mons CT: nDiff_vVel
Feuch CT: nDiff_cVel
Feuch CT: nDiff_vVel
Boign CT: nDiff_cVel
Boign CT: nDiff_vVel
Feuch MI: nDiff_cVel
Feuch MI: nDiff_vVel
Mons RT: nDiff_cVel
Mons RT: nDiff_vVel
Boign RT: nDiff_cVel
Boign RT: nDiff_vVel
Mons G: cDiff_cVel
Mons G: vDiff_cVel
Mons G: vDiff_vVel
Feuch F: cDiff_cVel
Feuch F: vDiff_cVel
Feuch F: vDiff_vVel
Boign NT: cDiff_cVel
Boign NT: vDiff_cVel
Boign NT: vDiff_vVel
0 1 2 3 4 5 6
Mean diffusionn (cm^2 yr^{-1})
0.0 0.1 0.2 0.3 0.4 0.5
Mean convection velocity (cm yr^{-1})
0 2 4 6 8 10 12
Annual erosion (t ha^{-1} yr^{-1})

Figure 4

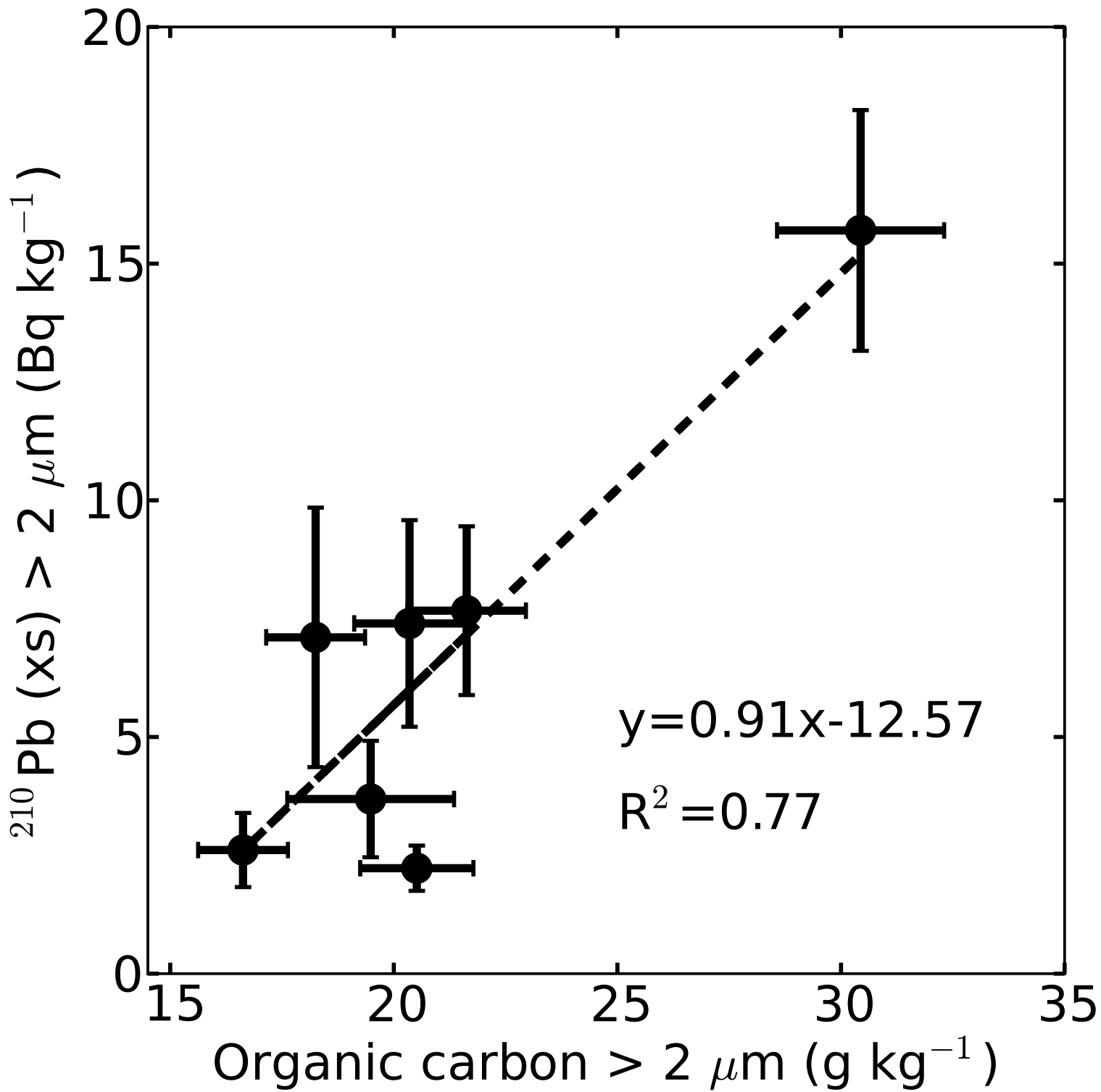
20
15
10
5
0
15
20
25
30
35
^{210}Pb (xs) > 2 μm (Bq kg^{-1})
Organic carbon > 2 μm (g kg^{-1})
y=0.91x-12.57
R^2=0.77

Figure 5

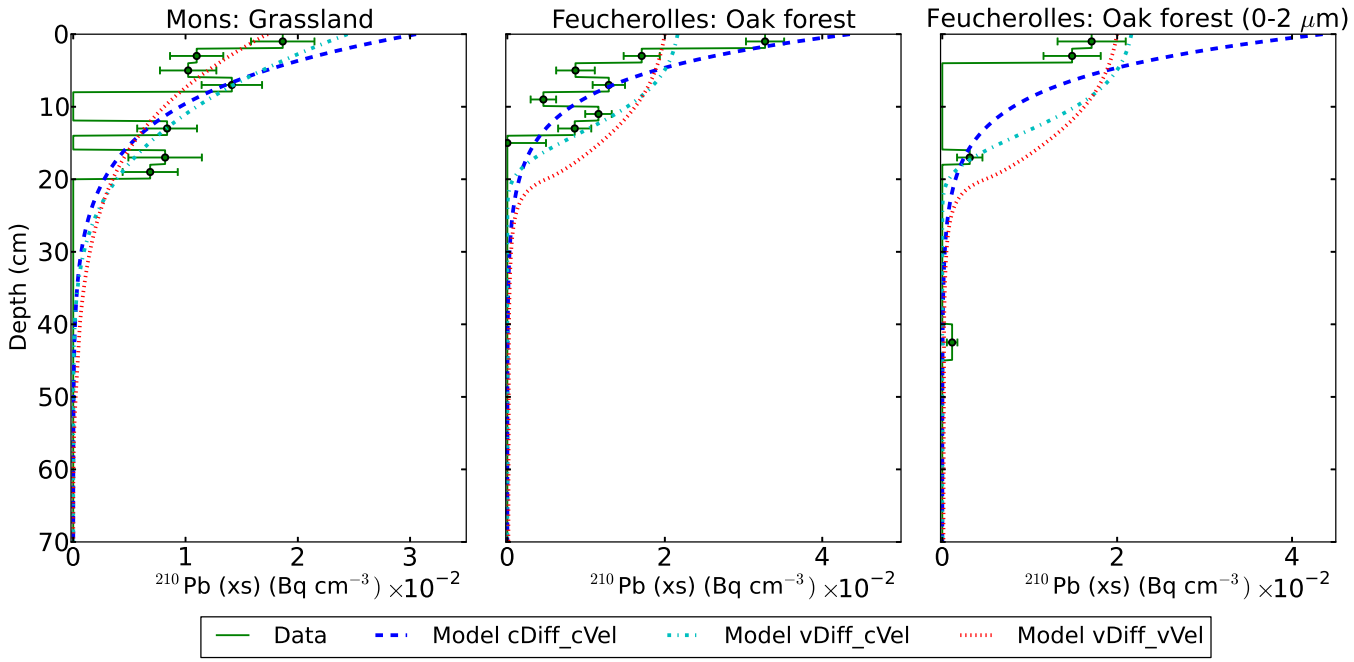
Mons: Grassland
Feucherolles: Oak forest
Feucherolles: Oak forest (0-2 μm)
Depth (cm)
0
10
20
30
40
50
60
70
0
1
2
3
0
2
4
0
2
4
^{210}Pb (xs) (Bq cm^{-3}) $\times 10^{-2}$
^{210}Pb (xs) (Bq cm^{-3}) $\times 10^{-2}$
^{210}Pb (xs) (Bq cm^{-3}) $\times 10^{-2}$
Data
Model cDiff_cVel
Model vDiff_cVel
Model vDiff_vVel

Supplementary Files

Click here to download Supplementary Files: AnnexA.docx